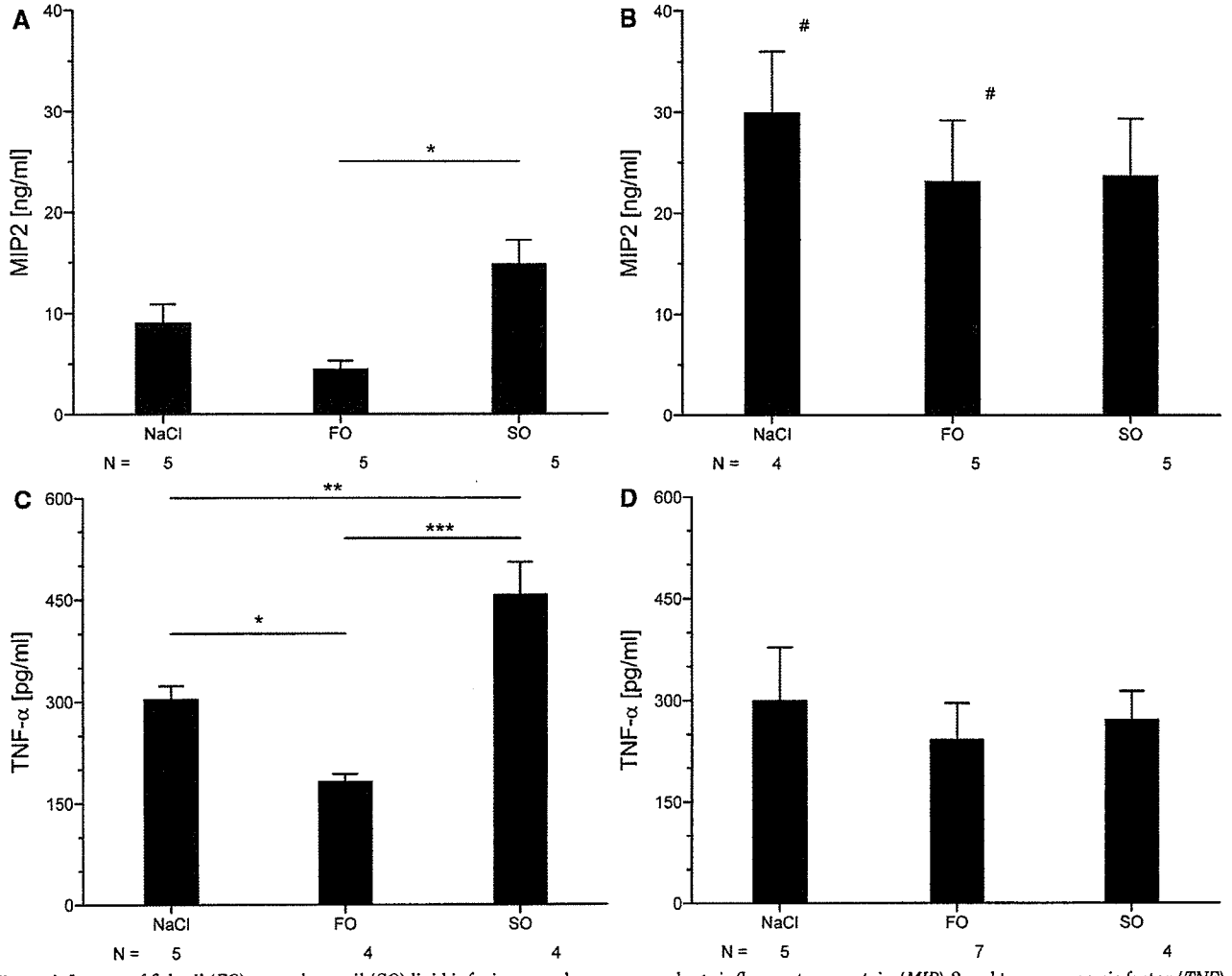

Figure 4. Impact of fish oil (*FO*) vs. soybean oil (*SO*) lipid infusions on plasma macrophage inflammatory protein (*MIP*)-2 and tumor necrosis factor (*TNF*)-α in wild-type (WT) mice and mice lacking the platelet-activating factor-receptor (PAF-R −/−) in a model of intraperitoneal inflammation. WT mice (*A, C*) or PAF-R−/− mice (*B, D*) were infused for 3 days with saline (control) or FO- or SO-based lipid emulsions, followed by stimulation with endotoxin (lipopolysaccharide, LPS) intraperitoneally 2 hrs before kill. MIP-2 (*A, B*) and TNF-α (*C, D*) in plasma were determined by enzyme-linked immunosorbent assay. Infusion of FO resulted in decreased MIP-2 formation in WT mice (*$p < .05$ vs. SO) but not in PAF-R−/− mice. TNF-α was increased after SO but decreased after FO compared with NaCl in WT mice receiving LPS (*$p < .05$; **$p < .01$; ***$p < .001$). MIP-2 was higher in PAF-R−/− mice after infusion with NaCl or FO compared with corresponding WT groups ($p < .01$). Data are given as mean ± SEM. Numbers of animals per group are detailed below columns.

model. These data are well in line with a previous report demonstrating regular responses of PAF-R −/− mice in an endotoxic shock model (15). Our data documenting elevated plasma levels of MIP-2 in PAF-R −/− mice compared with WT mice remain enigmatic. Elevated MIP-2 levels were observed both after lipid infusions and in saline controls. We speculate that this increase may be part of a long-term compensatory mechanism due to PAF-R deficiency, since PAF and MIP-2 may both act as chemoattractants. Further investigations are required to explain this phenomenon. In the PAF-RA group, the overall response to endotoxin remained intact. However, we found a delay in transmigration of leukocytes compared with WT mice: In mice receiving 10 μg of LPS, after 4 hrs leukocyte numbers were reduced but rose to an equal number of leukocytes after 24 hrs. Furthermore, we found a reduction of MIP2 and TNF-α in BAL in mice receiving 1 μg of LPS but not after 10 μg of endotoxin.

A striking finding of the present study was the differential impact of the FO vs. SO on cytokine generation provoked by endotoxin challenge in WT mice. In mice undergoing conventional SO-based lipid infusion, an augmentation of TNF-α and MIP-2 (the murine equivalent of interleukin-8) concentration in response to LPS challenge was observed irrespective of the model employed. In contrast, infusion of FO in WT mice resulted in reduced proinflammatory cytokine generation under all experimental conditions investigated. Although this is the first report of continuous lipid infusion in murine acute lung injury, our observations are consistent with previous findings demonstrating that TNF-α and interleukin-1 release was suppressed by dietary n-3 fatty acids in isolated murine splenocytes (25) and in isolated monocytes obtained from septic patients undergoing FO-based lipid infusions (18). Several days to weeks of oral FO supplementation are usually necessary to achieve such a change, whereas a

3-day infusion course sufficed to cause changes in cytokine synthesis in the present study and in patients receiving intravenous lipids (18). However using continuous enteral feeding, Gadek et al. (16) found a rapid increase in n-3 fatty acids in plasma phospholipids. We speculate that a key issue may be the continuous delivery of higher doses of FO to achieve fast changes. Preliminary data in our model suggest a rapid increase in n-3 fatty acids in plasma after infusion of FO and increase in n-6 polyunsaturated fatty acids in the SO group.

Pulmonary leukocyte recruitment was reduced in WT mice receiving FO-derived lipid emulsions. In contrast, SO-derived n-6 lipids increased leukocyte invasion and lung injury. We and others have described increased injury to lungs undergoing inflammatory stress due to n-6 lipids and, vice versa, an amelioration of damage by administration of n-3 lipids (26, 27). Mechanisms underlying this protective effect include, at least in part, the effect of FO on cytokine response described previously, generation of less potent lipid mediators as leukotriene B_5 instead of leukotriene B_4, formation of the less active vasoconstrictor thromboxane A_3 instead of thromboxane A_2, a reduction in platelet-activating factor synthesis, and reduced adhesion of leukocytes to endothelial cells (28–30). Transmigration of leukocytes through the endothelial-epithelial structures is a complex and tightly regulated process. The n-3 lipids interfere with this process at multiple stages, involving reduced presentation of endothelial adhesion molecules and reduced formation of platelet-activating factor by endothelial cells, which may then result in diminished activation of integrins on rolling leukocytes (28, 31). Furthermore, addition of arachidonic acid to endothelial cells increased thrombin-induced formation of PAF; in contrast, supplementation with n-3 fatty acids reduced its formation (28). As PAF generated by endothelial cells is not secreted to the supernatant but remains bound to the cell membrane, it may activate rolling leukocytes by binding to their PAF-R and initiate adhesion and transmigration (32). This mechanism may be at least in part responsible for the reduced rolling and adhesion of monocytes to endothelial cells after exposure to n-3 fatty acids and may translate in reduced transmigration of leukocytes (28).

Infusion of lipid emulsions bypasses physiologic uptake and processing of triglycerides by the gastrointestinal tract. Instead, infusion of synthetic lipid aggregates activates endothelial lipoprotein lipases, with translocation of the enzyme from its cellular binding sites into vascular compartment. Activation and translocation of this enzyme result in an increase in plasma free fatty acids due to avoidance of local cellular uptake mechanisms (33). The kinetics and duration of elevated plasma n-3 lipid levels thus exceed the corresponding alterations in response to conventional dietary FO uptake by orders of magnitude (34). Different availability of precursor fatty acids not only has an impact on subsequent generation of lipid mediators (e.g., substitution of leukotriene B_5 for B_4) but also reduces the generation of PAF due to incorporation into the phospholipid-precursor pool. In this respect, at least two lipid-dependent mechanisms may be relevant. First, enrichment of n-3 fatty acids in the PAF precursor pool may result in steric inhibition of phospholipase A_2 (32). Conversely, the increasing availability of arachidonic acid enhances generation of platelet-activating factor (28). Second, increasing n-3 fatty acids in phosphatidyl-inositol may impair the activation of leukocytes through reduction in intracellular second-messenger generation and activation of protein kinase C (7).

Recent experimental and clinical investigations suggest a strong link between the availability of free arachidonic acid, PAF, and lung injury. PAF and LPS promote lung injury and edema through sphingomyelinase-dependent formation of ceramide and activation of the cyclooxygenase pathway, which leads to the generation of arachidonic acid-derived prostanoids (35). Rapid infusion of conventional lipid emulsions in mechanically ventilated patients suffering from acute respiratory distress syndrome increased pulmonary shunt, notably linked to enhanced prostanoid generation resulting in a deterioration of the Pao_2/Fio_2 ratio (36). A second study in acute respiratory distress syndrome patients undergoing lipid infusions reported an increase in BAL PAF concentration and neutrophil counts paralleled by a deterioration in lung function, as measured by decreased Pao_2/Fio_2 (37). Despite these results and experimental use of PAF-RAs exhibiting beneficial properties in models of sepsis and acute lung injury (12, 38), phase III clinical studies using PAF-RAs or PAF-acetylhydrolase in septic patients have failed to show a difference in survival (13, 14). There may be a gap between experimental studies, when sepsis is initiated by a single LPS challenge with simultaneously started treatment, and clinical reality. Furthermore, as the response to LPS was intact in our model using PAF-R −/− mice, it remains to be determined if other inflammatory response systems may compensate for the inhibited PAF pathway.

However, the role of PAF in lipid infusion-related deterioration of lung function is underscored by our experiments using mice with a targeted disruption of the PAF receptor gene. Employing this strain, we were able to demonstrate that intratracheal LPS instillation provoked recruitment of leukocytes, as well as TNF-α and MIP-2 generation to the same extent as in WT mice, a phenomenon already described (15). Nevertheless, aggravation of lung inflammation by SO and its amelioration by FO-derived emulsions were essentially abolished in mice lacking this receptor. These results were confirmed in WT mice treated with a PAF-RA. Using BN52021, the differential impact of FO vs. SO on leukocyte recruitment and cytokine generation was also blocked. We conclude that major proinflammatory effects of conventional lipid emulsions and the ameliorating impact of FO-derived lipid emulsions on inflammation and pulmonary injury are linked to the integrity of PAF and PAF-R-related signaling in mice.

The correct timing and dosing of any pro- or anti-inflammatory drug in inflammation and sepsis are currently unsettled. N-3/n-6 ratios of 7.6:1 (FO) or 1:370 (safflower oil) have immune-suppressive features in a heart transplantation model (39), and application of SO (ratio 1:6.4) in septic patients increased the cytokine response (19). However, a ratio of 1:2 was shown to have only a minor impact on immunity in the heart transplantation model (39). Applying an n-3/n-6 ratio of 1:2 or 1:3 may therefore be a means to evade immune-modulating effects. Whereas FO in a hyperinflammatory state may be judged as an adjunct therapy, it may prove not to be beneficial in patients with already reduced immune response. Nevertheless, recent data from an observational study in 661 patients including 276 septic patients suggest that supplementation of parenteral nutrition with 0.1–0.2 g/kg/day FO had favorable effects on survival rate, infection rates, and length of stay in this subgroup (40). In addition, current studies using an enteral immune-modulating diet including n-3 fatty ac-

ids in patients with acute respiratory distress syndrome or sepsis show improvement in Pao_2/Fio_2 ratio, reduction in ventilation time, and even improvement in survival (16, 41, 42).

CONCLUSIONS

We demonstrated that infusion of FO-based lipid emulsions reduces LPS-induced proinflammatory cytokines, alveolar leukocyte transmigration, and protein leakage. In contrast, SO-based lipids lead to a further increase in the inflammatory response. However, the effect of lipid emulsions in murine inflammation is dependent on an intact PAF/PAF-R signaling. Administration of lipid emulsions not only may be regarded as a simple supply of calories but may also modulate the inflammatory response.

REFERENCES

1. Martin GS, Mannino DM, Eaton S, et al: The epidemiology of sepsis in the United States from 1979 through 2000. *N Engl J Med* 2003; 348:1546–1554
2. Brun-Buisson C, Minelli C, Bertolini G, et al: Epidemiology and outcome of acute lung injury in European intensive care units. Results from the ALIVE study. *Intensive Care Med* 2004; 30:51–61
3. Heller A, Koch T, Schmeck J, et al: Lipid mediators in inflammatory disorders. *Drugs* 1998; 55:487–496
4. Hotchkiss RS, Karl IE: The pathophysiology and treatment of sepsis. *N Engl J Med* 2003; 348:138–150
5. Mayer K, Schaefer MB, Seeger W: Fish oil in the critically ill: From experimental to clinical data. *Curr Opin Clin Nutr Metab Care* 2006; 9:140–148
6. Calder PC: Immunoregulatory and anti-inflammatory effects of n-3 polyunsaturated fatty acids. *Braz J Med Biol Res* 1998; 31: 467–490
7. Sperling RI, Benincaso AI, Knoell CT, et al: Dietary omega-3 polyunsaturated fatty acids inhibit phosphoinositide formation and chemotaxis in neutrophils. *J Clin Invest* 1993; 91:651–660
8. Denys A, Hichami A, Khan NA: n-3 PUFAs modulate T-cell activation via protein kinase C-alpha and -epsilon and the NF-kappaB signaling pathway. *J Lipid Res* 2005; 46: 752–758
9. Grimble RF, Howell WM, O'Reilly G, et al: The ability of fish oil to suppress tumor necrosis factor alpha production by peripheral blood mononuclear cells in healthy men is associated with polymorphisms in genes that influence tumor necrosis factor alpha production. *Am J Clin Nutr* 2002; 76:454–459
10. Zimmerman GA, McIntyre TM, Prescott SM, et al: The platelet-activating factor signaling system and its regulators in syndromes of inflammation and thrombosis. *Crit Care Med* 2002; 30:S294–S301
11. Leitinger N: Oxidized phospholipids as modulators of inflammation in atherosclerosis. *Curr Opin Lipidol* 2003; 14:421–430
12. Mathiak G, Szewczyk D, Abdullah F, et al: Platelet-activating factor (PAF) in experimental and clinical sepsis. *Shock* 1997; 7:391–404
13. Opal S, Laterre PF, Abraham E, et al: Recombinant human platelet-activating factor acetylhydrolase for treatment of severe sepsis: Results of a phase III, multicenter, randomized, double-blind, placebo-controlled, clinical trial. *Crit Care Med* 2004; 32: 332–341
14. Dhainaut JF, Tenaillon A, Hemmer M, et al: Confirmatory platelet-activating factor receptor antagonist trial in patients with severe gram-negative bacterial sepsis: A phase III, randomized, double-blind, placebo-controlled, multicenter trial. BN 52021 Sepsis Investigator Group. *Crit Care Med* 1998; 26: 1963–1971
15. Ishii S, Kuwaki T, Nagase T, et al: Impaired anaphylactic responses with intact sensitivity to endotoxin in mice lacking a platelet-activating factor receptor. *J Exp Med* 1998; 187:1779–1788
16. Gadek JE, DeMichele SJ, Karlstad MD, et al: Effect of enteral feeding with eicosapentaenoic acid, gamma-linolenic acid, and antioxidants in patients with acute respiratory distress syndrome. Enteral Nutrition in ARDS Study Group. *Crit Care Med* 1999; 27:1409–1420
17. Guarini P, Bellavite P, Biasi D, et al: Effects of dietary fish oil and soy phosphatidylcholine on neutrophil fatty acid composition, superoxide release, and adhesion. *Inflammation* 1998; 22:381–391
18. Mayer K, Gokorsch S, Fegbeutel C, et al: Parenteral nutrition with fish oil modulates cytokine response in patients with sepsis. *Am J Respir Crit Care Med* 2003; 167: 1321–1328
19. Mayer K, Meyer S, Reinholz-Muhly M, et al: Short-time infusion of fish oil-based lipid emulsions, approved for parenteral nutrition, reduces monocyte proinflammatory cytokine generation and adhesive interaction with endothelium in humans. *J Immunol* 2003; 171: 4837–4843
20. Maus UA, Koay MA, Delbeck T, et al: Role of resident alveolar macrophages in leukocyte traffic into the alveolar air space of intact mice. *Am J Physiol Lung Cell Mol Physiol* 2002; 282:L1245–L1252
21. Lowry OH, Rosebrough NJ, Farr AL, et al: Protein measurement with the Folin phenol reagent. *J Biol Chem* 1951; 193:265–275
22. Andonegui G, Bonder CS, Green F, et al: Endothelium-derived Toll-like receptor-4 is the key molecule in LPS-induced neutrophil sequestration into lungs. *J Clin Invest* 2003; 111:1011–1020
23. Parker JC, Townsley MI: Evaluation of lung injury in rats and mice. *Am J Physiol Lung Cell Mol Physiol* 2004; 286:L231–L246
24. Inoue K, Takano H, Shimada A, et al: Urinary trypsin inhibitor protects against systemic inflammation induced by lipopolysaccharide. *Mol Pharmacol* 2005; 67:673–680
25. Ishihara K, Komatsu W, Saito H, et al: Comparison of the effects of dietary alpha-linolenic, stearidonic, and eicosapentaenoic acids on production of inflammatory mediators in mice. *Lipids* 2002; 37:481–486
26. Grimminger F, Wahn H, Mayer K, et al: Impact of arachidonic versus eicosapentaenoic acid on exotonin-induced lung vascular leakage: Relation to 4-series versus 5-series leukotriene generation. *Am J Respir Crit Care Med* 1997; 155:513–519
27. Murray MJ, Kumar M, Gregory TJ, et al: Select dietary fatty acids attenuate cardiopulmonary dysfunction during acute lung injury in pigs. *Am J Physiol* 1995; 269: H2090–H2099
28. Mayer K, Merfels M, Muhly-Reinholz M, et al: Omega-3 fatty acids suppress monocyte adhesion to human endothelial cells: Role of endothelial PAF generation. *Am J Physiol Heart Circ Physiol* 2002; 283:H811–H818
29. Grimminger F, Mayer K, Kiss L, et al: PAF-induced synthesis of tetraenoic and pentaenoic leukotrienes in the isolated rabbit lung. *Am J Physiol Lung Cell Mol Physiol* 2000; 278:L268–L275
30. Murray MJ, Zhang T: The incorporation of dietary n-3 polyunsaturated fatty acids into porcine platelet phospholipids and their effects on platelet thromboxane A2 release. *Prostaglandins Leukot Essent Fatty Acids* 1997; 56:223–228
31. Weber C, Erl W, Pietsch A, et al: Docosahexaenoic acid selectively attenuates induction of vascular cell adhesion molecule-1 and subsequent monocytic cell adhesion to human endothelial cells stimulated by tumor necrosis factor-alpha. *Arterioscler Thromb Vasc Biol* 1995; 15:622–628
32. Prescott SM, Zimmerman GA, McIntyre TM: Platelet-activating factor. *J Biol Chem* 1990; 265:17381–17384
33. Peterson J, Bihain BE, Bengtsson-Olivecrona G, et al: Fatty acid control of lipoprotein lipase: A link between energy metabolism and lipid transport. *Proc Natl Acad Sci U S A* 1990; 87:909–913
34. Lovegrove JA, Brooks CN, Murphy MC, et al: Use of manufactured foods enriched with fish oils as a means of increasing long-chain n-3 polyunsaturated fatty acid intake. *Br J Nutr* 1997; 78:223–236
35. Goggel R, Winoto-Morbach S, Vielhaber G, et al: PAF-mediated pulmonary edema: A new role for acid sphingomyelinase and ceramide. *Nat Med* 2004; 10:155–160
36. Suchner U, Katz DP, Furst P, et al: Effects of intravenous fat emulsions on lung function in patients with acute respiratory distress syndrome or sepsis. *Crit Care Med* 2001; 29: 1569–1574

37. Lekka ME, Liokatis S, Nathanail C, et al: The impact of intravenous fat emulsion administration in acute lung injury. *Am J Respir Crit Care Med* 2004; 169:638–644
38. Christman BW, Lefferts PL, Blair IA, et al: Effect of platelet-activating factor receptor antagonism on endotoxin-induced lung dysfunction in awake sheep. *Am Rev Respir Dis* 1990; 142:1272–1278
39. Grimm H, Tibell A, Norrlind B, et al: Immunoregulation by parenteral lipids: Impact of the n-3 to n-6 fatty acid ratio. *JPEN J Parenter Enteral Nutr* 1994; 18:417–421
40. Heller AR, Rossler S, Litz RJ, et al: Omega-3 fatty acids improve the diagnosis-related clinical outcome. *Crit Care Med* 2006; 34:972–979
41. Singer P, Theilla M, Fisher H, et al: Benefit of an enteral diet enriched with eicosapentaenoic acid and gamma-linolenic acid in ventilated patients with acute lung injury. *Crit Care Med* 2006; 34:1033–1038
42. Pontes-Arruda A, Aragao AM, Albuquerque JD: Effects of enteral feeding with eicosapentaenoic acid, gamma-linolenic acid, and antioxidants in mechanically ventilated patients with severe sepsis and septic shock. *Crit Care Med* 2006; 34:2325–2333

THE JOURNAL OF BIOLOGICAL CHEMISTRY VOL. 282, NO. 8, pp. 5814–5824, February 23, 2007

LPA_4/p2y_9/GPR23 Mediates Rho-dependent Morphological Changes in a Rat Neuronal Cell Line*

Received for publication, June 21, 2006, and in revised form, December 15, 2006 Published, JBC Papers in Press, December 17, 2006, DOI 10.1074/jbc.M610767200

Keisuke Yanagida‡, Satoshi Ishii‡§1, Fumie Hamano‡, Kyoko Noguchi‡, and Takao Shimizu‡

From the ‡Department of Biochemistry and Molecular Biology, Faculty of Medicine, the University of Tokyo and the §Precursory Research for Embryonic Science and Technology (PRESTO) of Japan Science and Technology Agency, 7-3-1 Hongo, Bunkyo-ku, Tokyo 113-0033, Japan

Lysophosphatidic acid (LPA) is a potent lipid mediator that evokes a variety of biological responses in many cell types via its specific G protein-coupled receptors. In particular, LPA affects cell morphology, cell survival, and cell cycle progression in neuronal cells. Recently, we identified p2y_9/GPR23 as a novel fourth LPA receptor, LPA_4 (Noguchi, K., Ishii, S., and Shimizu, T. (2003) *J. Biol. Chem.* 278, 25600–25606). To assess the functions of LPA_4 in neuronal cells, we used rat neuroblastoma B103 cells that lack endogenous responses to LPA. In B103 cells stably expressing LPA_4, we observed $G_{q/11}$-dependent calcium mobilization, but LPA did not affect adenylyl cyclase activity. In LPA_4 transfectants, LPA induced dramatic morphological changes, *i.e.* neurite retraction, cell aggregation, and cadherin-dependent cell adhesion, which involved Rho-mediated signaling pathways. Thus, our results demonstrated that LPA_4 as well as LPA_1 couple to $G_{q/11}$ and $G_{12/13}$, whereas LPA_4 differs from LPA_1 in that it does not couple to $G_{i/o}$. Through neurite retraction and cell aggregation, LPA_4 may play a role in neuronal development such as neurogenesis and neuronal migration.

Lysophosphatidic acid (LPA,[2] 1- or 2-acyl-*sn*-glycero-3-phosphate) is a naturally occurring bioactive lipid mediator that controls growth, motility, and differentiation (1). LPA plays important roles in many biological processes, such as brain development, oncogenesis, wound healing, and immune functions (2). The effects of LPA on target cells are mediated by activation of its specific G protein-coupled receptors (GPCRs). The LPA_1 (3), LPA_2 (4), and LPA_3 (5) receptors are the major members of the endothelial differentiation gene (EDG) family that interact with LPA. Pharmacological studies suggest that both LPA_1 and LPA_2 couple to at least three types of G proteins, $G_{i/o}$, G_q, and $G_{12/13}$, whereas LPA_3 couples to $G_{i/o}$ and G_q but not $G_{12/13}$ (6). Depending on the functional coupling of a given LPA receptor to G proteins, LPA activates diverse signaling cascades involving phosphoinositide 3-kinase, phospholipase C, mitogen-activated protein kinase, Rho family GTPase, and adenylyl cyclase (2, 7).

LPA is present in the brain at relatively high levels compared with other organs (8, 9). LPA influences the cell morphology of several neuronal cell lines, neural progenitors, and primary neurons (10). It has also been reported that LPA affects electrophysiology, cell survival, and cell cycle progression in neuronal cells (10, 11). Targeted deletion of LPA_1 in mice produces olfactory deficits (12) and a behavioral abnormality (13). Furthermore, the use of LPA_1 knockouts revealed that LPA_1 is involved in the initiation of neuropathic pain (14). Exposure of the developing cerebral cortex to LPA produces dramatic changes in the folding of the brain, which do not occur in LPA_1 and LPA_2 double knockouts (15). However, the LPA receptor subtypes responsible for some neuronal effects have not been identified (16–18).

Recently, we identified p2y_9/GPR23 as a fourth LPA receptor (LPA_4) that is structurally distinct from the three LPA receptors of the EDG family (19). The expressed sequence tag cDNA encoding LPA_4 was originally isolated from human brain (20, 21), and LPA_4 expression has been detected in rat embryonic hippocampal neurons (22) and immortalized hippocampal progenitor cells (18). These facts suggest that LPA_4 may have important roles in neurodevelopmental processes such as neurogenesis and neuronal migration. However, only very limited information is available regarding its physiological and biological functions. To assess the functional roles of LPA_4 in neuronal cells, we generated B103 cells stably expressing LPA_4. This study demonstrates that treatment of the LPA_4-expressing cells with LPA leads to morphological changes, including cell rounding and cadherin-dependent cell adhesion following cell aggregation, both of which are mediated by the Rho/Rho-associated kinase (ROCK) pathway. The effects of LPA_4 on the morphology of the neuronal cells were clearly distinct from those of LPA_1, probably because LPA_4 does not couple to $G_{i/o}$.

EXPERIMENTAL PROCEDURES

Cell Culture—B103 rat neuroblastoma cells were kindly provided by Dr. J. Chun (The Scripps Research Institute, La Jolla, CA). B103 cells expressing each of the LPA receptors were maintained on poly-L-lysine-coated 100-mm dishes (Iwaki,

* This work was supported by grants-in-aid from the Ministry of Education, Culture, Sports, Science, and Technology of Japan (to T. S. and S. I.). The costs of publication of this article were defrayed in part by the payment of page charges. This article must therefore be hereby marked "*advertisement*" in accordance with 18 U.S.C. Section 1734 solely to indicate this fact.

[1] To whom correspondence should be addressed: Dept. of Biochemistry and Molecular Biology, Faculty of Medicine, The University of Tokyo, 7-3-1 Hongo, Bunkyo-ku, Tokyo 113-0033, Japan. Tel.: 81-3-5802-2925; Fax: 81-3-3813-8732; E-mail: mame@m.u-tokyo.ac.jp.

[2] The abbreviations used are: LPA, lysophosphatidic acid; GPCR, G protein-coupled receptor; EDG, endothelial differentiation gene; ROCK, Rho-associated kinase; DMEM, Dulbecco's modified Eagle's medium; PTX, pertussis toxin; HA, hemagglutinin; PBS, phosphate-buffered saline; BSA, bovine serum albumin; HBSS, Hank's balanced salt solution; IBMX, 2-isobutyl-1-methylxanthine; $[Ca^{2+}]_i$, intracellular Ca^{2+} concentration; EGFP, enhanced green fluorescence proteins; S1P, sphingosine 1-phosphate; MEMF, mouse embryonic meningeal fibroblast; MSF, mouse skin fibroblast.

Tokyo, Japan) in Dulbecco's modified Eagle's medium (DMEM) (Sigma) supplemented with 10% fetal bovine serum (BioWhittaker, Walkersville, MD) and 0.3 mg/ml G418 (Wako, Osaka, Japan). For some experiments, cells were pretreated with 100 ng/ml pertussis toxin (PTX) (List Biological Laboratories, Campbell, CA; from a 400 μg/ml stock in 10 mM Tris-HCl (pH 7.4) and 2 M urea stored at 4 °C) for 12 h, 5 μM YM-254890 (a novel $G_{q/11}$ inhibitor (23), a kind gift from Dr. J. Takasaki, Astellas Pharma Inc., Tokyo, Japan; from a 10 mM stock in dimethyl sulfoxide (Sigma) stored at −30 °C) for 10 min, or 5 μM Y-27632 (Calbiochem; from a 5 mM stock in water stored at −30 °C) for 10 min. Pretreatment with vehicles of PTX and YM-254890 was used as a control.

Stable Expression of LPA_1 and LPA_4—A DNA fragment containing the entire open reading frame of LPA_1 (NCBI accession number NM_001401) was first amplified from a cDNA prepared from human brain poly(A)$^+$ RNA (Clontech) by PCR using *Pfu* turbo DNA polymerase (Stratagene, La Jolla, CA) and oligonucleotides (sense primer, 5′-AAGAAAATTTGTCTCCCGTAGCTCT-3′ and antisense primer, 5′-CATGAGTTGACTTTTCTCCTCTCTC-3′). The entire open reading frame of LPA_1 with an additional sequence encoding a hemagglutinin (HA) epitope (YPYDVPDYA) at the 5′-end was subsequently amplified from the resultant PCR products using KOD-Plus DNA polymerase (Toyobo, Osaka, Japan) and oligonucleotides (sense primer containing the KpnI and HA tag sequences, 5′-GGGGTACCGCCATGTACCCCTACGACGTGCCCGACTACGCCGCTGCCATCTCTACTTCC-3′ and antisense primer containing the SpeI sequence, 5′-GGACTAGTCTAAACCACAGAGTGGTCATT-3′). The resultant DNA fragment was digested with KpnI and SpeI and subsequently cloned into the mammalian expression vector pCXN2.1, a slightly modified version of pCXN2 (24) with multiple cloning sites, between the KpnI and SpeI sites. HA-tagged human LPA_4 cDNA was constructed and cloned into pCXN2.1 as described previously (19). B103 cells were transfected using the Lipofectamine 2000 reagent (Invitrogen). After 48 h, the transient expression of the HA epitope on the cell surface was confirmed by flow cytometric analysis (EPICS XL, Beckman Coulter, Fullerton, CA) with the 3F10 rat monoclonal anti-HA antibody (Roche Applied Science) and phycoerythrin-labeled anti-rat IgG (Beckman Coulter) as the secondary antibody. Stable transfectants were selected with 1 mg/ml G418 for 26 days. After staining the drug-resistant cells as described above, a group of HA-positive cells was sorted by flow cytometry (EPICS ALTRA, Beckman Coulter) and maintained with 0.3 mg/ml G418. Three weeks later, a second round of sorting was performed; the twice-immunopurified cells were used for experiments (termed B103-LPA_1 and B103-LPA_4 cells).

Binding Assay—Binding assay was done essentially as described previously (19), with minor modifications. Cells (4×10^6) were seeded in collagen-coated 100-mm plates (Iwaki), followed by 24 h of serum starvation. The cells were washed with phosphate-buffered saline (PBS) twice and scraped off. After further washing with binding buffer (25 mM HEPES-NaOH (pH 7.4), 10 mM $MgCl_2$, and 0.25 M sucrose), the cells were suspended in the buffer with additional protease inhibitor mixture (Complete, Roche Applied Science), sonicated three times at 15 watts for 30 s, and centrifuged at 800 × *g* for 10 min at 4 °C. The supernatant was further centrifuged at $10^5 \times g$ for 60 min at 4 °C, and resultant pellet was homogenized in ice-cold binding buffer. Binding assays were performed in 96-well plates in triplicate. 20 μg each of the membrane fractions from the twice-immunopurified cells was incubated in binding buffer containing 0.25% bovine serum albumin (BSA) (fatty acid-free, very low endotoxin grade; Serologicals Proteins, Kankakee, IL) with 2-fold serial dilutions (50–3.125 nM) of [^{3}H]LPA (1-oleoyl[*oleoyl*-9,10-^{3}H]LPA, 57 Ci/mmol; PerkinElmer Life Sciences) for 60 min at 4 °C. The bound [^{3}H]LPA was collected onto a Unifilter-96-GF/C (PerkinElmer Life Sciences) using a MicroMate 196 harvester (Packard Instrument Co.). The filter was then rinsed 10 times with ice-cold binding buffer and dried for 12 h at 50 °C. 25 μl of MicroScint-0 scintillation mixture (PerkinElmer Life Sciences) was added per well. The radioactivity that remained on the filter was measured with TopCount microplate scintillation counter (Packard Instrument Co.). Total and nonspecific bindings were evaluated in the absence and presence of 10 μM unlabeled LPA [1-*oleoyl* (18:1)-LPA; Cayman Chemical, Ann Arbor, MI), respectively. The specific binding value (disintegrations/min) was calculated by subtracting the nonspecific binding value (disintegrations/min) from the total binding value (disintegrations/min). A dissociation constant (K_d) and a maximum binding capacity (B_{max}) were calculated by Scatchard analysis. B_{max} and K_d values for B103-LPA_1 cells were 0.8 pmol/mg protein and 18 nM, respectively. Those for B103-LPA_4 cells were 6.0 pmol/mg protein and 58 nM. No specific binding was observed in vector-transfected B103 cells (B103-vector cells).

cAMP Measurement—Cells (3.2×10^4) were seeded in collagen-coated 96-well plates (Iwaki), followed by 24 h of serum starvation. To determine whether LPA receptors mediate the inhibition of adenylyl cyclase, an AlphaScreen cAMP assay kit (PerkinElmer Life Sciences) was used as recommended in the manufacturer's instructions. The cells were washed twice with buffer A (Hanks' balanced salt solution (HBSS) containing 25 mM HEPES-NaOH (pH 7.4) and 0.1% BSA (Serologicals Proteins)) and incubated in 100 μl of buffer A containing 0.5 mM 3-isobutyl-1-methylxanthine (IBMX))(from a 20 mM stock in dimethyl sulfoxide stored at −30 °C) (Sigma) for 15 min at room temperature. The reaction was initiated by adding 50 μl of various concentrations of LPA in buffer A with 50 μM forskolin (Wako; from a 10 mM stock in dimethyl sulfoxide stored at −30 °C). After 30 min of incubation at room temperature, the reaction was terminated by adding 16.6 μl of 10% Tween 20, followed by overnight storage at 4 °C. After centrifugation at 800 × *g* for 5 min, the cAMP concentration in the supernatant was measured in quadruplicate with a fusion system (PerkinElmer Life Sciences). To determine whether LPA receptors mediate the stimulation of adenylyl cyclase, the cAMP Biotrak EIA system (Amersham Biosciences) was used as recommended in the manufacturer's instructions. The cells were washed twice with HEPES-Tyrode's buffer (25 mM HEPES-NaOH (pH 7.4), 140 mM NaCl, 2.7 mM KCl, 1 mM $CaCl_2$, 0.49 mM $MgCl_2$, 12 mM $NaHCO_3$, 0.37 mM NaH_2PO_4, and 5.6 mM D-glucose) containing 0.1% BSA (HEPES-Tyrode's BSA buffer) and incubated in 100 μl of HEPES-Tyrode's BSA buffer con-

taining 0.5 mM IBMX for 15 min at 37 °C. The reaction was initiated by adding 100 μl of various concentrations of LPA in HEPES-Tyrode's BSA buffer. After 30 min of incubation at 37 °C, the reaction was terminated by adding 25 μl of lysis buffer. Cell lysates in a volume of 100 μl were used to determine the cAMP concentration using an enzyme immunoassay method.

Ca^{2+} Measurement—Cells serum-starved for 24 h were detached with PBS containing 2 mM EDTA, washed with HEPES-Tyrode's buffer, and then loaded with 3 μM Fura-2 AM (Dojindo, Kumamoto, Japan) in HEPES-Tyrode's BSA buffer for 1 h at 37 °C. The cells were washed twice and resuspended in HEPES-Tyrode's BSA buffer at a density of 1×10^6 cells/ml. The cell suspension (0.5 ml) was applied to a CAF-100 spectrofluorometer (Jasco, Tokyo, Japan), and 5 μl of 100 μM LPA in HEPES-Tyrode's BSA buffer was added. The intracellular Ca^{2+} concentration ($[Ca^{2+}]_i$) was measured as the ratio of emission fluorescence at 500 nm in response to excitation at 340 and 380 nm.

Cell Rounding Assay—Cells (1×10^4) were seeded in poly-D-lysine-coated 12-well plates (BD Biosciences). After 24 h of incubation, the cells were washed three times with DMEM containing 0.1% BSA and serum-starved for 24 h. Three hours after a medium change, the cells were treated with 1 μM LPA for 15 min. The cells were examined for a round cell morphology lacking any neurite extensions or filopodia. Extended neurites were defined as having a length greater than the cell body. The number of rounded cells was expressed as a percentage of the observed cells (>200 cells/well).

Rho Inhibition Study—Cells (5×10^5) were seeded in poly-L-lysine-coated 35-mm dishes (Iwaki) in DMEM supplemented with 10% fetal bovine serum. After 24 h, either the *Clostridium botulinum* C3 exoenzyme expression vector (pEF-C3) (25) (a kind gift from Dr. S. Narumiya, Kyoto University, Kyoto, Japan) or the corresponding control vector (pEF-BOS) (26) (a kind gift from Dr. S. Nagata, Osaka University, Osaka, Japan) was cotransfected with an enhanced green fluorescent protein (EGFP) expression vector (pEGFP-C1; Clontech) at a 4:1 weight ratio, with 3 μg of total DNA, using the Lipofectamine 2000 reagent (Invitrogen). After 24 h, the cells were seeded in poly-D-lysine-coated 12-well plates and cultured for 24 h. The cells were then serum-starved for 12 h and treated with 1 μM LPA for 15 min. Following fixation with 1% paraformaldehyde for 15 min at 4 °C, EGFP images were obtained using a fluorescence microscope (Diaphoto, Nikon, Tokyo, Japan). EGFP-positive cells were examined for a round morphology without any neurite extensions or filopodia. At least 20 different fields were observed with a minimum of 100 EGFP-positive cells. The number of rounded cells was expressed as a percentage of the EGFP-positive cells.

Quantification of Cell Clustering—The degree of cell clustering was quantified by observing the distribution of the cell nuclei. Cells (1.5×10^5) were seeded in poly-D-lysine-coated 24-well plates (BD Biosciences). After 24 h of incubation, the cells were washed three times with DMEM containing 0.1% BSA and serum-starved for 24 h. Three hours after a medium change, the cells were treated with 1 μM LPA for 3 h, followed by fixation and staining with a Diff-Quik kit (Kokusai Shiyaku, Kobe, Japan). The distribution of the cells was mapped in rectangular areas (1710×1290 μm) by photographing the cultures (Cool Pix 990, Nikon). Each map was overlaid with grids at equal intervals (30 μm) and divided into 2451 unit squares. The randomness in spatial distribution was tested by counting the number of unit squares containing at least one nucleus. The intensity of the cell clustering was expressed as the percentage of the unit squares without any nuclei.

Cell Dissociation Assay—The Ca^{2+} sensitivity of cell-cell adhesion was estimated using trypsin treatment in the presence of either $CaCl_2$ (TC treatment) or EDTA (TE treatment) as described (27, 28), with minor modifications. Briefly, 5×10^5 cells were seeded in poly-D-lysine-coated 35-mm dishes (BD Biosciences) and cultured overnight. After 24 h of serum starvation, the cells were stimulated with 1 μM LPA for 2 h and washed with HBSS containing either 2 mM $CaCl_2$ or 2 mM EDTA. The washed cells were treated with 0.01% trypsin for 30 min at 37 °C and then dissociated by pipetting 10 times gently in 1 ml of HBSS with 0.01% trypsin. The number of cell clusters was counted with a particle counter (Beckman Coulter). The degree of cell-cell adhesion was expressed as the ratio of particles in the TC condition to particles in the TE condition (TC/TE). Negative control experiments without LPA treatment were also performed.

Western Blotting—Cells (4×10^6) were seeded in poly-L-lysine-coated 100-mm dishes. Following 24 h of serum starvation, the cells were treated with 1 μM LPA for 3 h, washed twice with PBS, and harvested in buffer B (25 mM HEPES-NaOH (pH 7.4), 10 mM $MgCl_2$, and 0.25 M sucrose). The cells were centrifuged at $800 \times g$ for 10 min at 4 °C, suspended in ice-cold buffer B containing 20 μM 4-amidinophenylmethylsulfonyl fluoride (Sigma) and a protease inhibitor mixture (Complete, Roche Applied Science), and sonicated three times for 30 s each at 4 °C. The cell debris was removed by centrifugation at $800 \times g$ for 10 min at 4 °C. The protein concentration of the homogenate was determined with a Bradford assay (Bio-Rad) using BSA as a standard. Five micrograms of protein sample containing 5% 2-mercaptoethanol was analyzed by 7.5% SDS-PAGE followed by transfer to a polyvinylidene difluoride membrane (Millipore Corp., Bedford, MA). The membrane was blocked with 5% skim milk (Difco) and probed with a mouse monoclonal antibody against N-cadherin or E-cadherin (BD Biosciences). The bands were visualized with an ECL chemiluminescence detection system (Amersham Biosciences) using horseradish peroxidase-conjugated anti-mouse IgG (Amersham Biosciences).

Immunofluorescence—Cells (3×10^5) were seeded into poly-L-lysine-coated glass-bottomed 35-mm dishes (Matsunami, Tokyo, Japan) and serum-starved for 24 h. Following stimulation with 1 μM LPA for 3 h at 37 °C, the cells were fixed with 4% paraformaldehyde for 20 min at 4 °C and rinsed twice with ice-cold PBS. Subsequently, the cells were incubated with a mouse monoclonal antibody against N-cadherin in PBS containing 1/4× permeabilization reagent (Beckman Coulter) for 1 h at room temperature. The primary antibody staining was visualized with an Alexa 488-conjugated goat anti-mouse IgG (Invitrogen). Images were obtained using an LSM510 laser-scanning confocal microscope (Carl Zeiss, Jena, Germany) equipped with an argon laser as the light source.

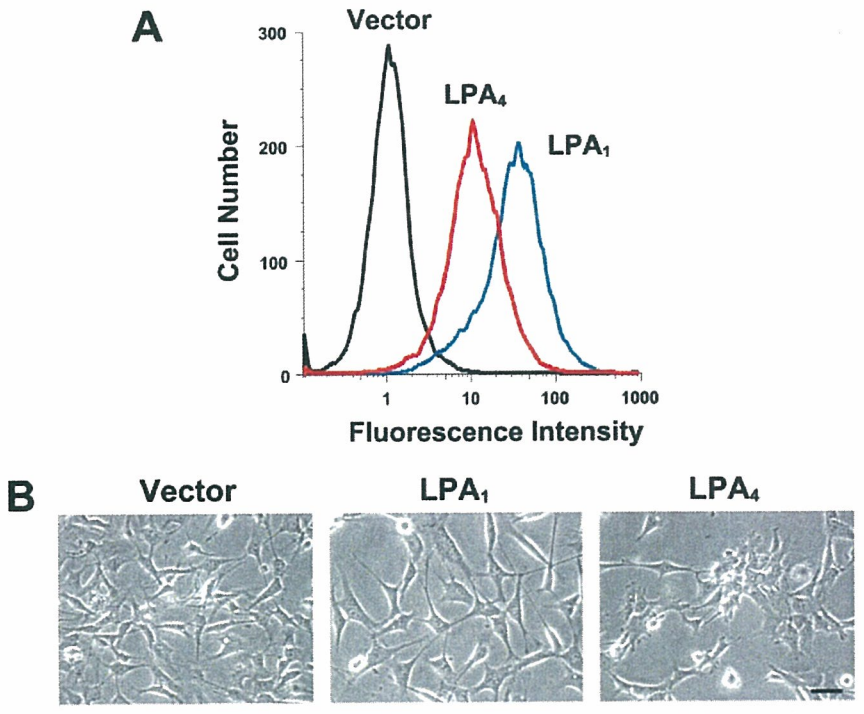

FIGURE 1. **Stable expression of LPA_1 or LPA_4 in B103 cells results in distinct morphologies.** *A*, flow cytometry analysis. B103 cells were stably transfected with the expression vectors for LPA_1 or LPA_4, each tagged with an HA epitope at the N terminus. After staining with an anti-HA antibody and a phycoerythrin-conjugated secondary antibody, HA-positive cells were sorted with a cell sorter and then subcultured. Data shown are the surface expression levels of the HA epitope in subcultured polyclonal cells obtained by the second round of cell sorting. Empty vector-transfected polyclonal cells served as a negative control. *B*, morphology of B103-vector, B103-LPA_1, and B103-LPA_4 cells in serum-containing medium. The cells were photographed 24 h after seeding. Each stable cell line showed similar growth rate. *Bar*, 40 μm.

Statistical Analysis—All values in the figures are expressed as means ± S.E. To determine statistical significance, the values were compared by analysis of variance followed by Tukey-Kramer test using Prism 4 software (GraphPad Software, San Diego, CA). The differences were considered significant if p values were less than 0.05.

RESULTS

Stable Expression of LPA_1 and LPA_4 in B103 Cells Results in Different Morphologies in Serum-containing Medium—To address the functional roles of LPA_4 in neuronal cells, B103 rat neuroblastoma cells were stably transfected with the expression vector for either LPA_1 or LPA_4. B103 cells were selected because they lack endogenous responses to LPA (29, 30). Consistently, no specific binding was observed in B103-vector cells in the radioligand binding assays (see "Experimental Procedures"). To determine the intrinsic gene expression profiles of LPA receptors in B103 cells, we performed a reverse transcription-PCR analysis of total cellular RNA from the cells. Although LPA_4 mRNA expression was slightly detected, no mRNA expression of the other three receptors, LPA_1, LPA_2, and LPA_3, was observed (data not shown). This finding is consistent with a recent report by Tsukahara *et al.* (31). The apparent discrepancy between the expression of LPA_4 and the lack of response to LPA might occur because the expression of LPA_4 is too low to respond to LPA. Alternatively, post-transcriptional/translational modifications (32) may produce discordance between mRNA and protein expression. Thus, we discounted the low expression of LPA_4 in B103 cells and took advantage of their unresponsiveness to LPA and their neuronal nature for the purpose of examining the functional roles of LPA_4 in neuronal cells.

For the construction of stably transfected cell lines, LPA_1 and LPA_4 were tagged with an HA epitope at the N terminus to enable us to determine the levels of expression on the cell surfaces. Fluorescence-activated cell sorting enriched a polyclonal population of the drug-resistant cells that expressed each LPA receptor. These populations of stable clones are free of any clonal deviation that could cause functional variations. Following two rounds of cell sorting, we observed that the fluorescence intensity of B103-LPA_1 cells was higher than that of B103-LPA_4 cells (Fig. 1*A*), although the B_{max} value for B103-LPA_1 cells (0.8 pmol/mg of protein) was lower than that for B103-LPA_4 cells (6.0 pmol/mg of protein). The apparent discrepancy might be because of two possibilities as follows: the usage of organellar membrane-rich microsome fractions and the difference in HA antibody immunoreactivity to the HA epitope tagged to two receptors. To confirm that no expression of the other subtypes of LPA receptors was enhanced secondary to the transfection, reverse transcription-PCR was performed with specific primers for LPA_1, LPA_2, LPA_3, and LPA_4 in B103-vector, B103-LPA_1, and B103-LPA_4 cells. As in the parental B103 cells, we observed only a low expression of LPA_4 and virtually no expression of the other LPA receptors in all of the transfected cell lines (data not shown).

Although these stably transfected cell lines showed similar growth rates (data not shown), they showed distinctly different morphologies in serum-containing medium (Fig. 1*B*). As reported previously (33), B103-LPA_1 cells displayed a flattened and more migratory morphology compared with B103-vector cells. Interestingly, B103-LPA_4 cells had an epithelial like morphology and appeared to adhere more tightly to each other than B103-vector cells. These observations suggest that LPA_1 and LPA_4 have distinct signaling pathways that produce different cell morphologies.

LPA_4 Does Not Affect Adenylyl Cyclase Activity in B103 Cells—We examined whether LPA_4 mediates the inhibition of adenylyl cyclase activity in B103 cells, as the other three LPA receptors do (30) (Fig. 2*A*). In B103-LPA_1 cells, LPA caused a dose-dependent inhibition of adenylyl cyclase activity with IC_{50} values below 10 nM (Fig. 2*A*). This inhibition was completely

blocked by PTX treatment, indicating the primary role of $G_{i/o}$ proteins. However, LPA at concentrations up to 10 μM did not blunt the forskolin-driven rises in cAMP accumulation in either B103-vector or B103-LPA$_4$ cells, suggesting that LPA$_4$ does not couple to $G_{i/o}$ proteins.

Previously, we reported that LPA induces cAMP accumulation in LPA$_4$-expressing Chinese hamster ovary cells (19). However, LPA did not elevate basal cAMP levels in either B103-LPA$_4$ cells or B103-LPA$_1$ cells (Fig. 2*B*), suggesting that neither LPA$_1$ nor LPA$_4$ couples to G_s in B103 cells.

LPA$_1$ and LPA$_4$ Mediate Ca^{2+} Mobilization via Distinct Signaling Pathways—LPA has been shown to induce intracellular Ca^{2+} mobilization in many cell types (34), and all EDG family LPA receptor subtypes mediate Ca^{2+} mobilization when expressed in B103 cells (30). We therefore examined whether LPA$_4$ mediates Ca^{2+} mobilization in B103 cells. Although B103-vector cells displayed no response to 1 μM LPA, increases in $[Ca^{2+}]_i$ were observed both in B103-LPA$_1$ and B103-LPA$_4$ cells (Fig. 3). LPA induces phospholipase C-mediated Ca^{2+} mobilization via the PTX-sensitive $G_{i/o}$- and/or PTX-insensitive $G_{q/11}$-mediated pathways (34). To examine the signaling pathways leading to Ca^{2+} mobilization in B103-LPA$_1$ and B103-LPA$_4$ cells, we treated the cells with a $G_{q/11}$-selective inhibitor, YM-254890 (23) (Fig. 3). ATP was used as a positive control, because ATP evokes Ca^{2+} mobilization via P2Y receptors predominantly through $G_{q/11}$ (35). The LPA-induced Ca^{2+} response in B103-LPA$_4$ cells and the ATP-induced Ca^{2+} response in both transfected cell lines were completely abolished by pretreatment with 5 μM YM-254890 (Fig. 3). In B103-LPA$_1$ cells, YM-254890 only partially inhibited the LPA-induced response (Fig. 3), but the combination of PTX and YM-254890 produced complete inhibition (data not shown). The degree of inhibition with YM-254890 in B103-LPA$_1$ cells was not altered at higher concentrations (up to 20 μM; data not shown), indicating that 5 μM YM-254890 was sufficient to inhibit the activation of $G_{q/11}$ proteins. These results suggest that both $G_{i/o}$ and $G_{q/11}$ proteins mediate Ca^{2+} mobilization in B103-LPA$_1$ cells, whereas $G_{q/11}$ is the dominant mediator of the response in B103-LPA$_4$ cells.

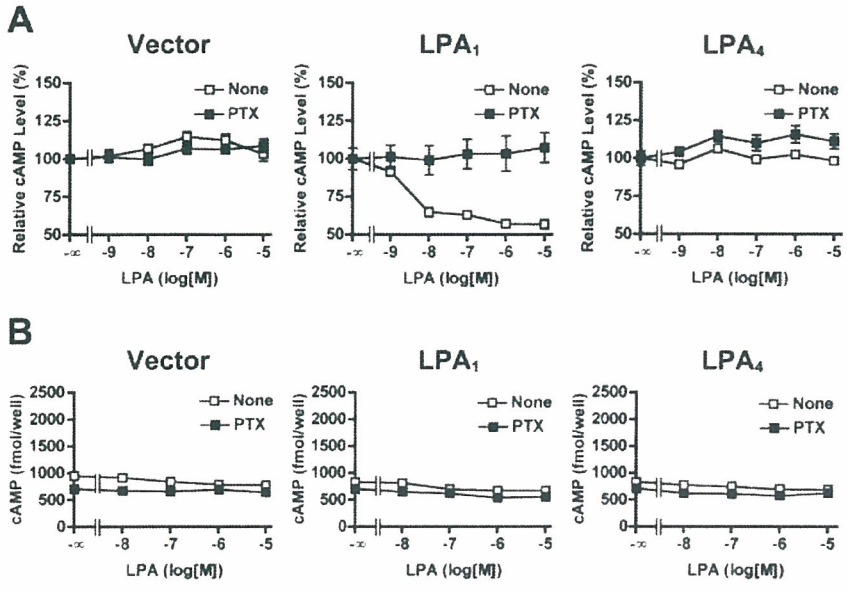

FIGURE 2. **LPA does not affect adenylyl cyclase activity in B103-LPA$_4$ cells.** *A*, failure of LPA to inhibit forskolin-induced cAMP accumulation in B103-LPA$_4$ cells. Serum-starved B103-vector, B103-LPA$_1$, and B103-LPA$_4$ cells were stimulated with increasing concentrations of LPA in the presence of 0.5 mM IBMX and 50 μM forskolin. After a 30-min incubation at room temperature, the cells were solubilized, and cAMP concentrations in the cell lysates were measured. Forskolin-induced cAMP accumulation in the absence of LPA was set to 100%. Where indicated, the cells were pretreated with 100 ng/ml PTX for 24 h. Data are means ± S.E. ($n = 4$) of a representative of three independent experiments with similar results. *B*, failure of LPA to induce cAMP accumulation in B103-LPA$_4$ cells. Serum-starved B103-vector, B103-LPA$_1$, and B103-LPA$_4$ cells were stimulated with increasing concentrations of LPA in the presence of 0.5 mM IBMX. After a 30-min incubation at room temperature, the cells were solubilized, and cAMP concentrations in the cell lysates were measured. The cells were pretreated with 100 ng/ml PTX for 24 h. Data are representative of three independent experiments with similar results.

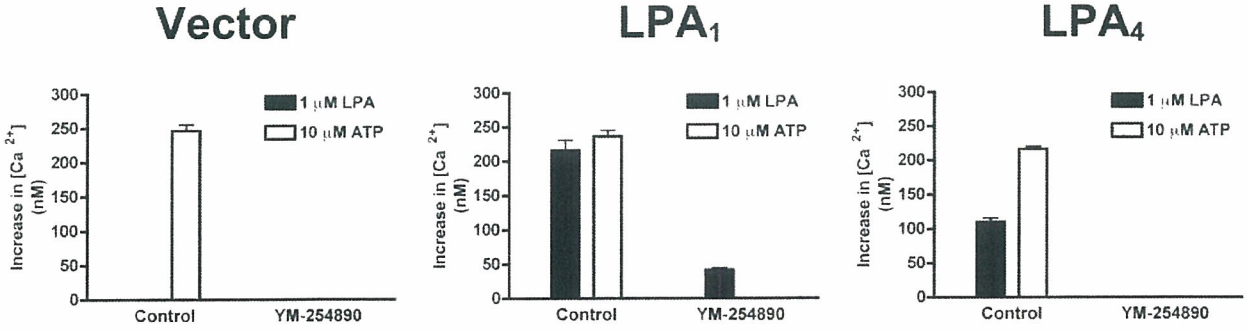

FIGURE 3. **LPA$_4$-mediated Ca^{2+} mobilization is entirely dependent on $G_{q/11}$ proteins.** B103-vector, B103-LPA$_1$, and B103-LPA$_4$ cells were serum-starved, loaded with 3 μM Fura-2 AM, and stimulated with 1 μM LPA or 10 μM ATP. Where indicated, the cells were pretreated with 5 μM YM-254890 for 10 min. Data are means ± S.E. ($n = 3$) of a representative of three independent experiments with similar results.

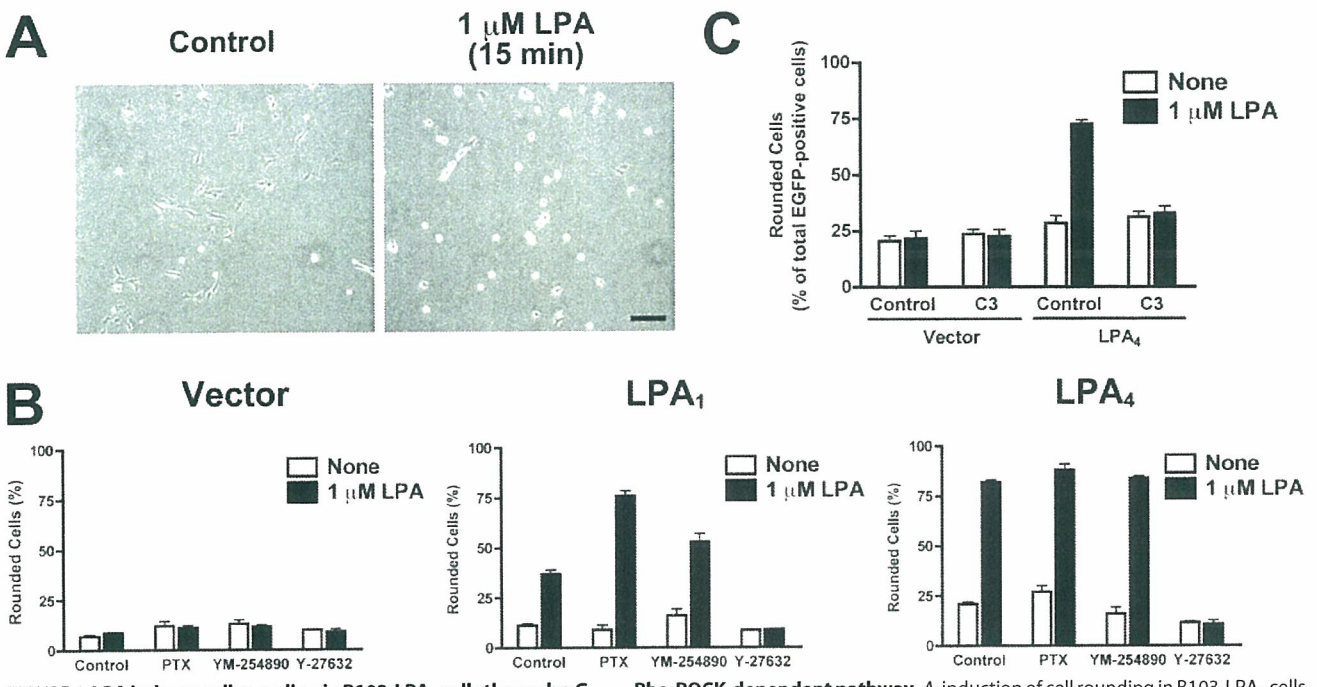

FIGURE 4. **LPA induces cell rounding in B103-LPA_4 cells through a $G_{12/13}$-Rho-ROCK-dependent pathway.** *A*, induction of cell rounding in B103-LPA_4 cells. Serum-starved B103-LPA_4 cells were stimulated with 1 μM LPA for 15 min. *Bar*, 100 μm. *B*, effects of PTX, YM-254890, and Y-27632 on LPA-induced cell rounding in B103-vector, B103-LPA_1, and B103-LPA_4 cells. The cells were pretreated with either 100 ng/ml PTX for 24 h, 5 μM YM-254890 for 10 min, or 5 μM Y-27632 for 10 min. The percentages of rounded cells among >200 cells are shown. Data are means ± S.E. (n = 3) of a representative of three independent experiments with similar results. *C*, effects of C3 exoenzyme on LPA-induced cell rounding in B103-LPA_4 cells. Either the C3 exoenzyme expression vector or the corresponding control vector was cotransfected with the EGFP expression vector. The cells were seeded, serum-starved, and treated with 1 μM LPA for 15 min. Following the fixation, EGFP images were obtained using a fluorescence microscope. The percentages of rounded cells among >100 EGFP-positive cells are shown. Data are means ± S.E. (n = 3) of a representative of two independent experiments with similar results.

(10). Mouse LPA_1 and LPA_2 and human LPA_1 have been reported to mediate LPA-induced cell rounding in B103 cells (29, 30, 33); we examined whether human LPA_4 also mediates cell rounding in B103 cells by seeding cells at a low cell density (Fig. 4, *A* and *B*). Overexpression of LPA_1 and LPA_4 slightly increased the percentages of rounded cells even before LPA application. Within 15 min of LPA stimulation, about 80% of B103-LPA_4 cells became rounded and underwent neurite retraction (Fig. 4*A*). Cell rounding was observed in B103-LPA_1 cells as reported previously (33), but to a lesser degree than in B103-LPA_4 cells. LPA-induced cell rounding was not observed in B103-vector cells.

The role of Rho in LPA-induced cell rounding is now well established (36), and the $G_{12/13}$ types of heterotrimeric G proteins are known to be upstream activators of Rho proteins (1, 2, 7). On the other hand, there are reports that $G_{q/11}$ activation induces cell rounding through Rho-dependent (37) and -independent (38) pathways. To determine which G proteins and signaling molecules are involved in LPA-induced cell rounding, we pretreated the cells with PTX, YM-254890, and a ROCK inhibitor, Y-27632 (Fig. 4*B*). In B103-LPA_4 cells, neither PTX nor YM-254890 inhibited LPA-induced cell rounding; in contrast, Y-27632 completely inhibited this morphological change. Y-27632 also hampered LPA-induced cell rounding in B103-LPA_1 cells, whereas YM-254890 did not affect the number of rounded cells. Interestingly, pretreatment with PTX increased the degree of LPA-induced cell rounding in B103-LPA_1 cells. To confirm the involvement of Rho, B103-LPA_4 cells were transfected with C3 exoenzyme, which inactivates Rho by ADP-ribosylation. The transfected cells were identified by cotransfection of an EGFP expression construct. C3 exoenzyme transfection blunted LPA-induced cell rounding in B103-LPA_4 cells, again indicating the involvement of Rho (Fig. 4*C*).

LPA_4 Mediates ROCK-dependent Cell Aggregation—As described earlier, B103-LPA_4 cells appeared to form aggregates in serum-containing medium to a greater extent than B103-vector cells (Fig. 1*B*). To determine whether the binding of LPA to LPA_4 mediates the induction of cell-cell adhesion, B103-LPA_4 cells at a medium cell density were stimulated with 1 μM LPA after 24 h of serum starvation. Although the rapid cell rounding after LPA application was difficult to evaluate at this cell density because of the formation of cell-cell contacts, LPA caused a slow but dramatic aggregation in B103-LPA_4 cells (Fig. 5*A*, *panel f*). The morphological change observed in B103-LPA_4 cells was transient, reaching a maximum 2–3 h after the treatment and then returning to the base line 24 h after the treatment (data not shown).

To investigate the signaling pathways downstream of LPA_4 that are involved in the cell aggregation, we treated B103-LPA_4 cells with several inhibitors. The LPA-induced morphological changes in B103-LPA_4 cells were completely prevented by Y-27632 (Fig. 5*A*, *panel o*). In contrast, neither PTX nor YM-254890 inhibited the cell aggregation (Fig. 5*A*, *panels i* and *l*). We quantified the degree of cell aggregation by examining the randomness in the spatial distribution of the cells (see the "Experimental Procedures"; Fig. 5*B*). These results suggest that

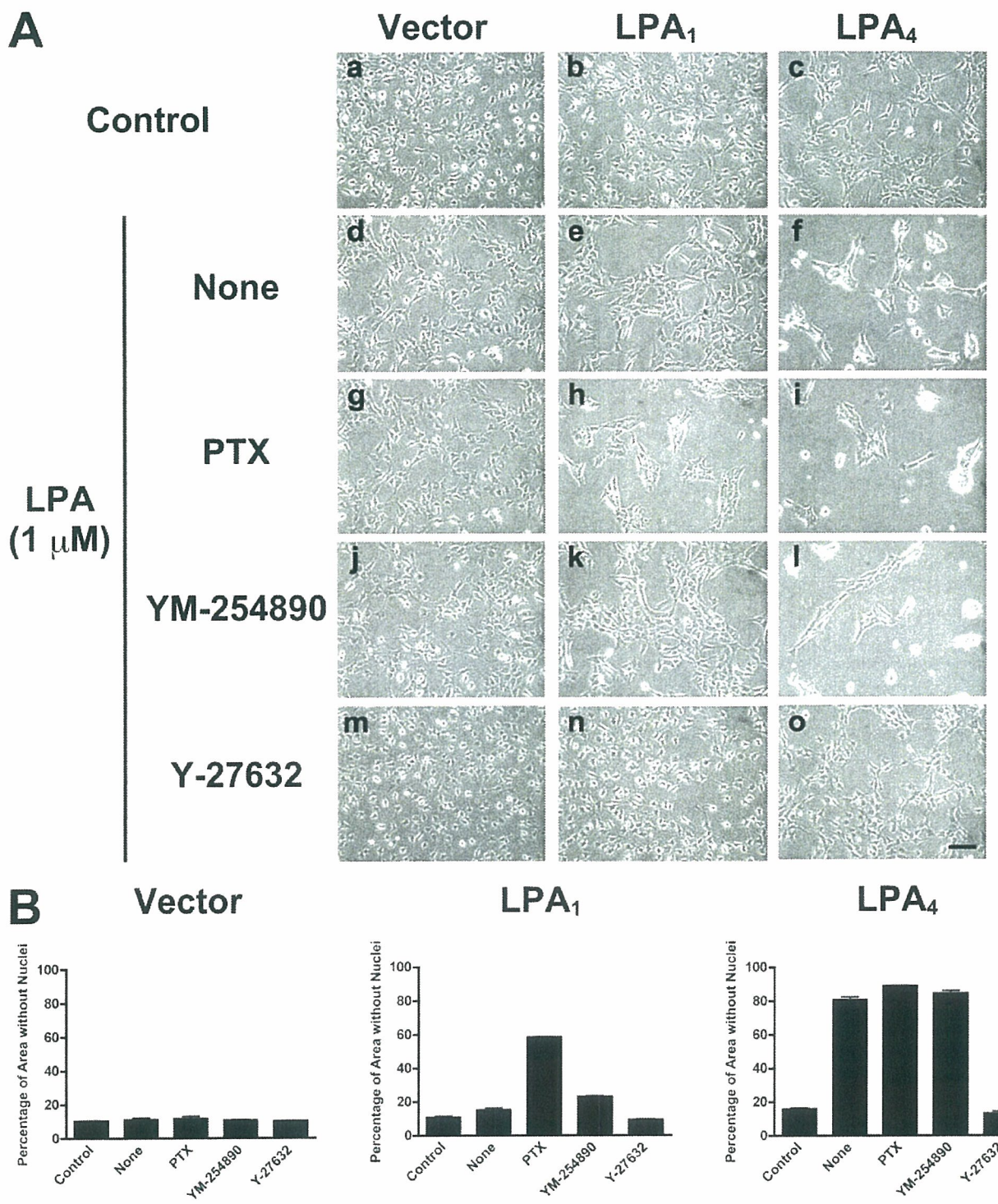

FIGURE 5. **Cell aggregation in B103-LPA$_4$ cells is mediated by ROCK.** *A*, cells were pretreated with either 100 ng/ml PTX for 24 h, 5 μM YM-254890 for 10 min, or 5 μM Y-27632 for 10 min prior to the LPA stimulation for 3 h. *Bar*, 100 μm. *B*, quantification of cell clustering. Serum-starved cells were treated with 1 μM LPA for 3 h, followed by fixation and staining. The intensity of the cell clustering was calculated as described under the "Experimental Procedures." Data are means ± S.E. of three different rectangular areas (one rectangular area/well) of two independent experiments with similar results.

Rho mediates LPA-induced cell aggregation in B103-LPA$_4$ cells in a $G_{i/o}$- and $G_{q/11}$-independent manner. Rho regulates the reorganization of the actin cytoskeleton, which can modify the intensity of adhesion (28, 39). To examine whether the reorganization of the actin cytoskeleton was involved in this effect, B103-LPA$_4$ cells were pretreated with cytochalasin D (an inhibitor of actin polymerization). In these cells, morphological changes were not observed after LPA stimulation, indicating that actin reorganization is involved in the LPA-induced cell aggregation (data not shown). Like B103-LPA$_4$ cells, PTX-

treated B103-LPA_1 cells became aggregated after LPA stimulation (Fig. 5*A*, *panel h*).

LPA_4 Mediates N-cadherin-dependent Cell-Cell Adherence—Through LPA-induced cell aggregation, B103-LPA_4 cells formed tightly compact aggregates (Fig. 5*A*, *panel f*), which dissociated very little after pipetting (data not shown). Cell-cell adhesion mechanisms can be Ca^{2+}-dependent and Ca^{2+}-independent, and cadherins are the major components of the Ca^{2+}-dependent system. Cadherin-dependent adhesion was originally defined as being trypsin-resistant in the presence of Ca^{2+} and trypsin-sensitive in the absence of Ca^{2+} (40). We examined whether LPA-induced cell adhesion was mediated by cadherins using a cell dissociation assay, one of the adhesion assays for the evaluation of the cadherin activity (27, 28). We defined the TC/TE index as a ratio of the cell particle number after trypsin treatment in the presence of Ca^{2+} (TC) to the number after trypsin treatment with EDTA (TE). Cadherin-dependent adhesion remains after trypsin-Ca^{2+} treatment, whereas trypsin-EDTA treatment disrupts cell adhesion nearly completely. In either treatment, an increase in particles would occur when a large aggregate breaks into small particles by pipetting; the higher the number of particles, the lower the aggregation (adhesion). Thus, the TC/TE index is negatively correlated with cadherin-mediated adhesion. The aggregation level of B103-LPA_4 cells increased after LPA stimulation (Fig. 6*A*; note that the index inversely reflects cadherin activity). LPA treatment did not significantly affect the TC/TE index in either B103-vector cells or B103-LPA_1 cells. These results suggest that LPA increased the cadherin-mediated adhesive activity in B103-LPA_4 cells. Even LPA-untreated B103-LPA_4 cells had significantly more cadherin-dependent adhesion activity, *i.e.* a lower TC/TE index, than LPA-untreated B103-vector and B103-LPA_1 cells (Fig. 6*A*).

The cadherins constitute a large superfamily of molecules that includes the classic cadherins, the desmosomal cadherins, the protocadherins, and the cadherin-like signaling receptors (41). The levels of the two classic cadherins most commonly expressed in the nervous system, N- and E-cadherin, were determined by Western blotting of LPA-treated or -untreated B103 cells. Consistent with a previous report (42), these cells abundantly expressed N-cadherin (Fig. 6*B*), whereas E-cadherin was undetectable (data not shown). The expression level of N-cadherin was not up-regulated by LPA treatment in any of the transfected cell lines (Fig. 6*B*), and N-cadherin was intact in the cells undergoing TC treatment. In contrast, TE treatment resulted in complete digestion of N-cadherin (data not shown), as reported previously (43). We next examined whether LPA increases N-cadherin-mediated cell-cell contacts. LPA promoted the assembly of N-cadherin in the form of a thick, bright band at the cell-cell contact area in B103-LPA_4 cells but not in B103-vector cells (Fig. 6*C*).

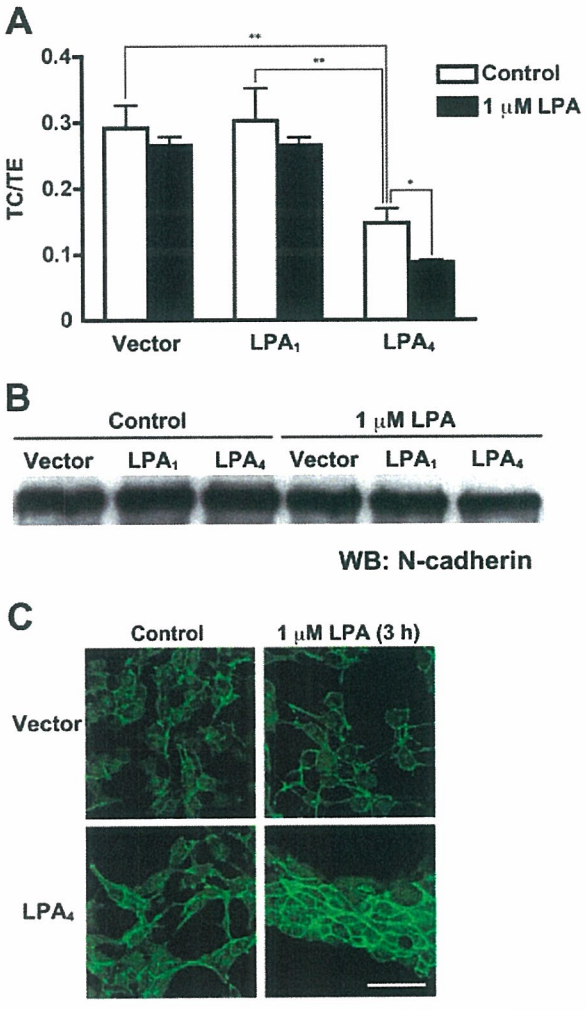

FIGURE 6. **LPA induces N-cadherin-dependent cell adhesion in B103-LPA_4 cells.** *A*, Ca^{2+} dependence of cell-cell adhesion in B103-LPA_4 cells. Serum-starved cells were stimulated with 1 μM LPA for 2 h and washed with HBSS containing either 1 mM Ca^{2+} or 1 mM EDTA. The washed cells were treated with 0.01% trypsin for 30 min in the presence of either Ca^{2+} (TC treatment) or EDTA (TE treatment) at 37 °C. Then the cells were dissociated by pipetting 10 times, and the number of particles was counted with a particle counter. The degree of cell-cell adhesion was expressed as the ratio of TC/TE. Note that the ratio inversely reflects cadherin activity. Negative control experiments without LPA treatment were also performed. Data are means ± S.E. of five independent experiments. *, $p < 0.05$; **, $p < 0.001$ (using analysis of variance followed by Tukey-Kramer test). *B*, expression of N-cadherin protein in B103 cells. Serum-starved cells were incubated with or without 1 μM LPA for 3 h and lysed. The same amount of protein was subjected to Western blot (*WB*) analysis. *C*, immunostaining of N-cadherin in B103-vector and B103-LPA_4 cells. Serum-starved cells were stimulated with 1 μM LPA, stained with an antibody against N-cadherin, and visualized with a fluorescein-labeled secondary antibody. Negative control experiments without LPA treatment were also performed. *Bar*, 100 μm.

DISCUSSION

A number of studies have shown that LPA mediates morphological changes in neuronal cells through the Rho-ROCK pathway (10, 11, 44). It has been proposed that these effects are mediated by LPA_1 and/or LPA_2 (10, 11, 44). Recently, we identified $p2y_9$/GPR23 as a fourth LPA receptor (LPA_4) that is structurally distinct from the EDG family of LPA receptors (19). The expression of LPA_4 in neuronal cells implies a significant role for this receptor in the nervous system (18). The results in this study demonstrate that LPA_4 caused morphological changes in B103 neuronal cells, including cell rounding and N-cadherin-associated cell aggregation, both of which were mediated by the Rho-ROCK pathway.

Ca^{2+} mobilization and adenylyl cyclase inhibition are the major cellular responses to LPA (45). When expressed in B103

neuronal cells, each of the EDG family LPA receptors, LPA_1, LPA_2, and LPA_3, mediates both of these reactions (30). LPA_1 is likely to mediate the Ca^{2+} response through $G_{q/11}$ proteins (Fig. 3). The PTX-sensitive inhibition of adenylyl cyclase (Fig. 2*A*) suggests that LPA_1 also couples to $G_{i/o}$. We showed that LPA_4 mediates the Ca^{2+} response in B103 cells (Fig. 3). This is consistent with our previous report (19) that the stable expression of LPA_4 in Chinese hamster ovary cells significantly enhanced the LPA-induced Ca^{2+} mobilization. From our results using YM-254890, LPA_4 probably mediates Ca^{2+} mobilization through $G_{q/11}$ proteins (Fig. 3). In contrast, LPA did not inhibit adenylyl cyclase in B103-LPA_4 cells (Fig. 2*A*). These results indicate that unlike the other LPA receptor subtypes, LPA_4 does not couple to $G_{i/o}$ proteins.

Neurite retraction and neurite formation play a role in the remodeling of neurons for guidance and synaptic plasticity (46). Neurite retraction in neuronal cells is induced by lysophospholipids, including LPA and sphingosine 1-phosphate (S1P), in addition to semaphorins, netrins, and ephrins (10, 11, 47). LPA induces neurite retraction through LPA_1 or LPA_2 when expressed in B103 cells (30). In this study, we showed that 1 μM LPA induced cell rounding in B103-LPA_4 cells (Fig. 4*A*). Sugiura *et al.* (48) reported that rat brain contains 3.73 nmol of LPA/g of tissue. These results suggest a role for LPA_4 in LPA-induced neurite retraction. Neurite initiation and formation involve actin cytoskeletal changes, and as a regulator of actin reorganization, Rho GTPase has a profound effect on neuritogenesis (47). For example, S1P induces Rho-dependent neurite retraction through the $S1P_2$ (49, 50), $S1P_3$ (49), and $S1P_5$ receptors (50, 51). Several studies have also revealed a critical role for Rho and ROCK in LPA-induced neurite retraction (36, 52, 53), although some studies have reported Rho-independent neurite retraction (38, 54). Judging from its complete inhibition by C3 exoenzyme and Y-27632, the cell rounding induced by LPA_4 depended on Rho and ROCK in B103-LPA_4 cells (Fig. 4, *B* and *C*).

In general, activation of $G_{12/13}$ proteins leads to an increase in RhoA guanine nucleotide exchange, activation of ROCK, and actin polymerization (55, 56), although some studies have implied that $G_{q/11}$ proteins can also activate Rho (57, 58). Based on our results, it is conceivable that the $G_{12/13}$ proteins are upstream regulators of Rho in B103-LPA_1 cells and B103-LPA_4 cells, because YM-254890 inhibited cell rounding in both cell types (Fig. 4*B*). In many studies reporting the induction of neurite retraction by LPA (10), the LPA receptor subtypes responsible have not been identified, or LPA_1 and LPA_2 were suggested as candidate subtypes based on mRNA expression in the neuronal cells examined (59–62). This study suggests the possibility that LPA_4 was involved in the neurite retraction in some of these studies.

LPA has been shown to stimulate cell motility and to modulate tumor cell invasion, both of which are mediated mainly by LPA_1 and $G_{i/o}$ proteins (33, 63, 64). In the presence of serum, B103-LPA_1 cells exhibited a flattened morphology and were widely dispersed throughout the dish (Fig. 1*B*) (33). This morphological phenotype was probably evoked by LPA through the LPA_1-$G_{i/o}$-Rac signaling axis (33). In sharp contrast to B103-LPA_1 cells, B103-LPA_4 cells formed cell aggregates in serum-containing medium (Fig. 1*B*), apparently through activation of the $G_{12/13}$-Rho-ROCK signaling axis (Fig. 5). This cell-cell adhesion involved N-cadherin without *de novo* synthesis (Fig. 6). Because Rho affects cadherin-dependent adhesion through actin cytoskeleton reorganization (28), we presume that LPA-induced cytoskeletal changes affect the subcellular distribution of N-cadherin, as shown in Fig. 6*C*, leading to strong cell-cell adhesion in B103-LPA_4 cells. This is supported by the current results that treatment with Y-27632 and cytochalasin D abolished the LPA-induced cell aggregation (Fig. 5 and data not shown). N-cadherin is widely expressed in the nervous system and has critical roles in neural development and functions, including synapse formation and myelination. Weiner *et al.* (65) previously reported that LPA induced cell-cell junctions containing N-cadherin in rat Schwann cells. Furthermore, LPA was reported to induce cell clustering in neural progenitor cells prepared from embryonic rat hippocampus (66) and in mouse postmitotic cortical neurons (16). Our results raise the possibility that in addition to LPA_1 and LPA_2, LPA_4 might also be involved in these effects in neural cells and have critical roles in the development and function of the nervous system. In contrast to LPA_1 and LPA_2, which activate Rac through $G_{i/o}$ (17, 64), LPA_4 is unlikely to activate the $G_{i/o}$-Rac pathway because LPA_4 did not inhibit adenylyl cyclase activity (Fig. 3*A*). Therefore, LPA_4 might have a unique role in keeping a proper balance between Rho and Rac activation, which is important for neuronal development and function (47).

We observed that PTX significantly enhanced the intensity of LPA_1-mediated cell rounding (Fig. 4*B*). This "permissive effect" is consistent with a previous report that PTX enables LPA-induced cell rounding in 1321N1 astrocytoma cells (61). It is known that Rho activity is inhibited by Rac activation through $G_{i/o}$ proteins (67). Indeed, Rac activation functionally antagonizes Rho-mediated neurite retraction in 1321N1 astrocytoma cells (61). LPA_1 was shown to couple to $G_{i/o}$ and activate Rac strongly in B103 cells (33) and other cells, including mouse embryonic meningeal fibroblast (MEMF) and mouse skin fibroblast (MSF) cells (17, 64). Taken together, we suggest that PTX treatment of B103-LPA_1 cells suppresses $G_{i/o}$ proteins and subsequently suppresses Rac activation by LPA, which in turn permits Rho-mediated cell rounding. This mechanism probably also accounts for the LPA-induced aggregation of PTX-treated B103-LPA_1 cells (Fig. 5, *A*, *panel h*, and *B*).

We showed here that LPA_4 has Rho-dependent morphological effects. It has been reported that LPA-induced Rho activation is mediated by LPA_1 and/or LPA_2. However, pathways independent of LPA_1 and LPA_2 have also been proposed. Contos *et al.* (17) showed that MEMF cells from LPA_1 and LPA_2 double knockouts remained capable of forming stress fibers in response to LPA. This study proposed the presence of unknown LPA receptors in MEMF cells because of the absence of LPA_3 mRNA. Consistent with this, Hama *et al.* (64) reported that LPA activates Rho in MSF cells from LPA_1 and LPA_2 double knockouts. Our results, together with the abundant expression of LPA_4 in MSF cells (64), suggest that LPA_4 may also be involved in LPA-induced Rho activation in these cells. Furthermore, Hama *et al.* (64) observed that Rac activation was totally

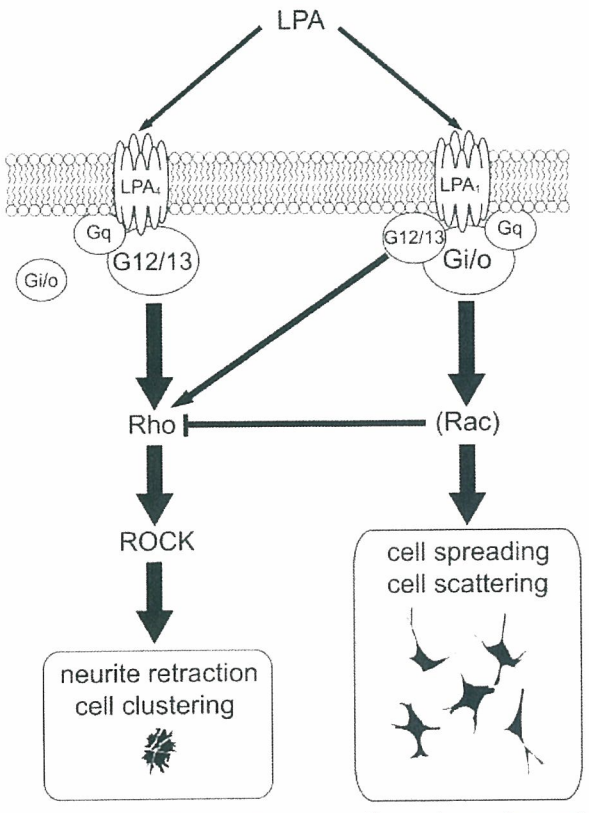

FIGURE 7. **LPA_1 and LPA_4 have distinct signaling pathways that produce different cell morphologies in B103 cells.** LPA_4 expression results in cell rounding and aggregated morphology through $G_{12/13}$-Rho-ROCK pathway. In contrast, LPA_1 expression results in flattened and dispersed morphology as reported previously (33). Inactivation of $G_{i/o}$ proteins in LPA_1-expressing cells by PTX treatment leads to "LPA_4-expressing cells like" aggregated morphology, suggesting the involvement of the inhibitory effect of $G_{i/o}$ on Rho activation probably through Rac. Both LPA_1 and LPA_4 couple to G_q, although G_q-involved pathway does not affect cell morphology.

dependent on LPA_1 and LPA_2, supporting our hypothesis that LPA_4 does not activate the $G_{i/o}$-Rac signaling axis.

We also observed that the stable expression of LPA_1 or LPA_4 slightly increased the population of rounded cells even before LPA application (Fig. 4*B*). Furthermore, serum-starved B103-LPA_4 cells adhered to one another more strongly than B103-vector or B103-LPA_1 cells did (Fig. 6*A*). These morphological effects might be because of the constitutive activation of these LPA receptors. Indeed, there are many reports showing that the constitutive expression of GPCR for lipid mediators, including lysophospholipids and prostanoids, has morphological effects (30, 49, 68, 69). For example, cell rounding and cadherin-dependent adhesion in the absence of ligand occur in human embryonic kidney 293 cells transfected with FP_B receptor, an isoform of prostanoid GPCR (69, 70). The involvement of phosphatidylinositol 3-kinase and β-catenin was proposed for these constitutive activities (70). Another conceivable explanation for the morphological effects observed in serum-starved B103-LPA_1 and B103-LPA_4 cells involves autocrine ligand secretion and subsequent receptor activation (33). Both hypotheses are consistent with our results that the treatment of these cells with Y-27632 decreased the percentage of rounded cells (Fig. 4*B*).

LPA_4 Changes the Morphology of Neuronal Cells

In summary, as shown in Fig. 7, we demonstrate for the first time that the novel LPA receptor subtype LPA_4 is coupled to the activation of Rho in a rat neuronal cell line. The activation of Rho through LPA_4 leads to morphological changes, including cell rounding and cell aggregation. LPA is well known to induce neurite retraction and cell clustering in neural cells. The identification of Rho as an effector of LPA_4 will give insight into some of the physiological and morphological effects of LPA that could not be explained by the EDG family LPA receptors. A full understanding of the potential roles of the endogenous LPA_4 receptor in the development and function of the nervous system awaits future studies.

Acknowledgments—We thank Drs. T. Yokomizo and T. Okuno (Kyushu University) for vital discussions and critical suggestions. We also thank Dr. J. Chun (The Scripps Research Institute, La Jolla, CA) for providing B103 rat neuroblastoma cells; Dr. J. Miyazaki (Osaka University) for pCXN2; Drs. S. Narumiya (Kyoto University) and S. Nagata (Osaka University) for the expression vector for C3 exoenzyme (pEF-C3) and its parental vector (pEF-BOS), respectively; and Dr. J. Takasaki (Astellas Pharma, Tokyo, Japan) for YM-254890.

REFERENCES

1. Moolenaar, W. H., van Meeteren, L. A., and Giepmans, B. N. (2004) *BioEssays* **26,** 870–881
2. Anliker, B., and Chun, J. (2004) *J. Biol. Chem.* **279,** 20555–20558
3. Hecht, J. H., Weiner, J. A., Post, S. R., and Chun, J. (1996) *J. Cell Biol.* **135,** 1071–1083
4. An, S., Bleu, T., Zheng, Y., and Goetzl, E. J. (1998) *Mol. Pharmacol.* **54,** 881–888
5. Bandoh, K., Aoki, J., Hosono, H., Kobayashi, S., Kobayashi, T., Murakami-Murofushi, K., Tsujimoto, M., Arai, H., and Inoue, K. (1999) *J. Biol. Chem.* **274,** 27776–27785
6. Contos, J. J., Ishii, I., and Chun, J. (2000) *Mol. Pharmacol.* **58,** 1188–1196
7. Ishii, I., Fukushima, N., Ye, X., and Chun, J. (2004) *Annu. Rev. Biochem.* **73,** 321–354
8. Das, A. K., and Hajra, A. K. (1989) *Lipids* **24,** 329–333
9. Tokumura, A. (1995) *Prog. Lipid Res.* **34,** 151–184
10. Ye, X., Fukushima, N., Kingsbury, M. A., and Chun, J. (2002) *Neuroreport* **13,** 2169–2175
11. Chun, J. (2005) *Prostaglandins Other Lipid Mediat.* **77,** 46–51
12. Contos, J. J., Fukushima, N., Weiner, J. A., Kaushal, D., and Chun, J. (2000) *Proc. Natl. Acad. Sci. U. S. A.* **97,** 13384–13389
13. Harrison, S. M., Reavill, C., Brown, G., Brown, J. T., Cluderay, J. E., Crook, B., Davies, C. H., Dawson, L. A., Grau, E., Heidbreder, C., Hemmati, P., Hervieu, G., Howarth, A., Hughes, Z. A., Hunter, A. J., Latcham, J., Pickering, S., Pugh, P., Rogers, D. C., Shilliam, C. S., and Maycox, P. R. (2003) *Mol. Cell. Neurosci.* **24,** 1170–1179
14. Inoue, M., Rashid, M. H., Fujita, R., Contos, J. J., Chun, J., and Ueda, H. (2004) *Nat. Med.* **10,** 712–718
15. Kingsbury, M. A., Rehen, S. K., Contos, J. J., Higgins, C. M., and Chun, J. (2003) *Nat. Neurosci.* **6,** 1292–1299
16. Fukushima, N., Weiner, J. A., Kaushal, D., Contos, J. J., Rehen, S. K., Kingsbury, M. A., Kim, K. Y., and Chun, J. (2002) *Mol. Cell. Neurosci.* **20,** 271–282
17. Contos, J. J., Ishii, I., Fukushima, N., Kingsbury, M. A., Ye, X., Kawamura, S., Brown, J. H., and Chun, J. (2002) *Mol. Cell. Biol.* **22,** 6921–6929
18. Jin Rhee, H., Nam, J. S., Sun, Y., Kim, M. J., Choi, H. K., Han, D. H., Kim, N. H., and Huh, S. O. (2006) *Neuroreport* **17,** 523–526
19. Noguchi, K., Ishii, S., and Shimizu, T. (2003) *J. Biol. Chem.* **278,** 25600–25606
20. Janssens, R., Boeynaems, J. M., Godart, M., and Communi, D. (1997) *Biochem. Biophys. Res. Commun.* **236,** 106–112
21. O'Dowd, B. F., Nguyen, T., Jung, B. P., Marchese, A., Cheng, R., Heng, H. H., Kolakowski, L. F., Jr., Lynch, K. R., and George, S. R. (1997) *Gene*

(*Amst.*) **187,** 75–81
22. Fujiwara, Y., Sebok, A., Meakin, S., Kobayashi, T., Murakami-Murofushi, K., and Tigyi, G. (2003) *J. Neurochem.* **87,** 1272–1283
23. Takasaki, J., Saito, T., Taniguchi, M., Kawasaki, T., Moritani, Y., Hayashi, K., and Kobori, M. (2004) *J. Biol. Chem.* **279,** 47438–47445
24. Niwa, H., Yamamura, K., and Miyazaki, J. (1991) *Gene* (*Amst.*) **108,** 193–199
25. Fujisawa, K., Madaule, P., Ishizaki, T., Watanabe, G., Bito, H., Saito, Y., Hall, A., and Narumiya, S. (1998) *J. Biol. Chem.* **273,** 18943–18949
26. Mizushima, S., and Nagata, S. (1990) *Nucleic Acids Res.* **18,** 5322
27. Nagafuchi, A., Ishihara, S., and Tsukita, S. (1994) *J. Cell Biol.* **127,** 235–245
28. Fukata, M., Kuroda, S., Nakagawa, M., Kawajiri, A., Itoh, N., Shoji, I., Matsuura, Y., Yonehara, S., Fujisawa, H., Kikuchi, A., and Kaibuchi, K. (1999) *J. Biol. Chem.* **274,** 26044–26050
29. Fukushima, N., Kimura, Y., and Chun, J. (1998) *Proc. Natl. Acad. Sci. U. S. A.* **95,** 6151–6156
30. Ishii, I., Contos, J. J., Fukushima, N., and Chun, J. (2000) *Mol. Pharmacol.* **58,** 895–902
31. Tsukahara, T., Tsukahara, R., Yasuda, S., Makarova, N., Valentine, W. J., Allison, P., Yuan, H., Baker, D. L., Li, Z., Bittman, R., Parrill, A., and Tigyi, G. (2006) *J. Biol. Chem.* **281,** 3398–3407
32. Bockaert, J., and Pin, J. P. (1999) *EMBO J.* **18,** 1723–1729
33. van Leeuwen, F. N., Olivo, C., Grivell, S., Giepmans, B. N., Collard, J. G., and Moolenaar, W. H. (2003) *J. Biol. Chem.* **278,** 400–406
34. Meyer Zu Heringdorf, D. (2004) *J. Cell. Biochem.* **92,** 937–948
35. von Kugelgen, I. (2006) *Pharmacol. Ther.* **110,** 415–432
36. Jalink, K., van Corven, E. J., Hengeveld, T., Morii, N., Narumiya, S., and Moolenaar, W. H. (1994) *J. Cell Biol.* **126,** 801–810
37. Katoh, H., Aoki, J., Yamaguchi, Y., Kitano, Y., Ichikawa, A., and Negishi, M. (1998) *J. Biol. Chem.* **273,** 28700–28707
38. Couvillon, A. D., and Exton, J. H. (2006) *Cell. Signal.* **18,** 715–728
39. Hall, A. (1998) *Science* **279,** 509–514
40. Takeichi, M. (1977) *J. Cell Biol.* **75,** 464–474
41. Gumbiner, B. M. (2005) *Nat. Rev. Mol. Cell Biol.* **6,** 622–634
42. Chen, Q., Chen, T. J., Letourneau, P. C., Costa Lda, F., and Schubert, D. (2005) *J. Neurosci.* **25,** 281–290
43. Wanner, I. B., and Wood, P. M. (2002) *J. Neurosci.* **22,** 4066–4079
44. Fukushima, N. (2004) *J. Cell. Biochem.* **92,** 993–1003
45. Tigyi, G. (2001) *Prostaglandins Other Lipid Mediat.* **64,** 47–62
46. Luo, L., and O'Leary, D. D. (2005) *Annu. Rev. Neurosci.* **28,** 127–156
47. Govek, E. E., Newey, S. E., and Van Aelst, L. (2005) *Genes Dev.* **19,** 1–49
48. Sugiura, T., Nakane, S., Kishimoto, S., Waku, K., Yoshioka, Y., Tokumura, A., and Hanahan, D. J. (1999) *Biochim. Biophys. Acta* **1440,** 194–204
49. van Brocklyn, J. R., Tu, Z., Edsall, L. C., Schmidt, R. R., and Spiegel, S. (1999) *J. Biol. Chem.* **274,** 4626–4632
50. Toman, R. E., Payne, S. G., Watterson, K. R., Maceyka, M., Lee, N. H., Milstien, S., Bigbee, J. W., and Spiegel, S. (2004) *J. Cell Biol.* **166,** 381–392
51. Jaillard, C., Harrison, S., Stankoff, B., Aigrot, M. S., Calver, A. R., Duddy, G., Walsh, F. S., Pangalos, M. N., Arimura, N., Kaibuchi, K., Zalc, B., and Lubetzki, C. (2005) *J. Neurosci.* **25,** 1459–1469
52. Hirose, M., Ishizaki, T., Watanabe, N., Uehata, M., Kranenburg, O., Moolenaar, W. H., Matsumura, F., Maekawa, M., Bito, H., and Narumiya, S. (1998) *J. Cell Biol.* **141,** 1625–1636
53. Kranenburg, O., Poland, M., van Horck, F. P., Drechsel, D., Hall, A., and Moolenaar, W. H. (1999) *Mol. Biol. Cell* **10,** 1851–1857
54. Somlyo, A. P., and Somlyo, A. V. (2000) *J. Physiol.* (*Lond.*) **522,** 177–185
55. Hart, M. J., Jiang, X., Kozasa, T., Roscoe, W., Singer, W. D., Gilman, A. G., Sternweis, P. C., and Bollag, G. (1998) *Science* **280,** 2112–2114
56. Kozasa, T., Jiang, X., Hart, M. J., Sternweis, P. M., Singer, W. D., Gilman, A. G., Bollag, G., and Sternweis, P. C. (1998) *Science* **280,** 2109–2111
57. Chikumi, H., Vazquez-Prado, J., Servitja, J. M., Miyazaki, H., and Gutkind, J. S. (2002) *J. Biol. Chem.* **277,** 27130–27134
58. Vogt, S., Grosse, R., Schultz, G., and Offermanns, S. (2003) *J. Biol. Chem.* **278,** 28743–28749
59. Sayas, C. L., Avila, J., and Wandosell, F. (2002) *J. Neurosci.* **22,** 6863–6875
60. Dawson, J., Hotchin, N., Lax, S., and Rumsby, M. (2003) *J. Neurochem.* **87,** 947–957
61. Seasholtz, T. M., Radeff-Huang, J., Sagi, S. A., Matteo, R., Weems, J. M., Cohen, A. S., Feramisco, J. R., and Brown, J. H. (2004) *J. Neurochem.* **91,** 501–512
62. Sayas, C. L., Moreno-Flores, M. T., Avila, J., and Wandosell, F. (1999) *J. Biol. Chem.* **274,** 37046–37052
63. Yamada, T., Sato, K., Komachi, M., Malchinkhuu, E., Tobo, M., Kimura, T., Kuwabara, A., Yanagita, Y., Ikeya, T., Tanahashi, Y., Ogawa, T., Ohwada, S., Morishita, Y., Ohta, H., Im, D. S., Tamoto, K., Tomura, H., and Okajima, F. (2004) *J. Biol. Chem.* **279,** 6595–6605
64. Hama, K., Aoki, J., Fukaya, M., Kishi, Y., Sakai, T., Suzuki, R., Ohta, H., Yamori, T., Watanabe, M., Chun, J., and Arai, H. (2004) *J. Biol. Chem.* **279,** 17634–17639
65. Weiner, J. A., Fukushima, N., Contos, J. J., Scherer, S. S., and Chun, J. (2001) *J. Neurosci.* **21,** 7069–7078
66. Harada, J., Foley, M., Moskowitz, M. A., and Waeber, C. (2004) *J. Neurochem.* **88,** 1026–1039
67. Burridge, K., and Wennerberg, K. (2004) *Cell* **116,** 167–179
68. Hasegawa, H., Negishi, M., Katoh, H., and Ichikawa, A. (1997) *Biochem. Biophys. Res. Commun.* **234,** 631–636
69. Pierce, K. L., Fujino, H., Srinivasan, D., and Regan, J. W. (1999) *J. Biol. Chem.* **274,** 35944–35949
70. Fujino, H., Srinivasan, D., and Regan, J. W. (2002) *J. Biol. Chem.* **277,** 48786–48795

第48回日本老年医学会学術集会記録
〈ミニレビュー〉

COPDガイドラインを高齢者診療にどう生かすか

長瀬　隆英

日本老年医学会雑誌　第43巻　第5号　別刷

第48回日本老年医学会学術集会記録
〈ミニレビュー〉

COPDガイドラインを高齢者診療にどう生かすか

長瀬　隆英

Key words：GOLDガイドライン，喫煙，吸入気管支拡張薬，インフルエンザワクチン
（日老医誌　2006；43：602-603）

はじめに

21世紀を迎えた現在，高齢者呼吸器疾患の社会的重要性は急増しつつあり，WHOによれば2020年の死亡要因の第3位がCOPD（慢性閉塞性肺疾患：chronic obstructive pulmonary disease）と予想されている．さてCOPDの重要性が医学界や政府に十分認識されていないことを懸念した科学者が中心となり，米国国立心肺血液研究所（NHLBI）とWHOの参加のもと，Global Initiative for Chronic Obstructive Lung Disease（GOLD）という組織が発足した．現在では，このGOLDガイドラインが国際的統一ガイドラインとなっている．今回はこのGOLDガイドラインを用いた高齢者診療について概説する．

COPDガイドラインの現況

1）概要

COPDは，日本呼吸器学会のガイドラインによれば，「有毒な粒子やガスの吸入によって生じた肺の炎症反応に基づく進行性の気流制限を呈する疾患」と定義されている．また，国際的にも，COPDに対する統一ガイドラインであるGlobal Initiative for Chronic Obstructive Lung Disease（GOLD）により，同様に定義されている．

世界的には，COPDは疾患別死因の第4位となっており，COPD患者数はさらに増大しつつある．また，COPDに対する医療コストの増加（米国では年間4兆円と見積もられている）も重要な課題とされる．COPDに対する医療費は，症状が進むにつれ急激に増加することが指摘されており，「早期に適格な」治療介入を行うことは社会的にも大きな利益があると考えられる．

2）病因，病態生理，発生機序

COPDの病因として最も重要なものが，喫煙である．喫煙者におけるCOPD発症率は年齢とともに増加する．COPDは，肺胞，末梢気道，中枢気道の全ての病変を包括するが，気流制限の主たる原因は末梢気道病変である．

3）症状

典型的なCOPDの患者は喫煙歴を有する高齢者であり，そのような患者が慢性の咳，慢性の痰，労作時の呼吸困難を有している場合にはCOPDがまず疑われる．この際，COPDにおける呼吸困難感は持続性・進行性のものであるため，特に高齢者においては，上記の症状を加齢によるものと考える傾向があるため，早期発見には注意深く問診をする必要がある．

COPDが疑われる患者においては，喫煙・職業・環境因子等のリスクファクター，喘息・アレルギー疾患・鼻茸などの既往，急性増悪の既往について十分注意した問診が必要である．また，βブロッカーなどの服薬歴にも注意を要する．

4）検査と診断

理学所見については，典型的には胸郭前後径の拡大，口すぼめ呼吸，聴診上肺音の減弱などが知られているが，これらがみられなくてもCOPDを否定することはできない．また，胸部X線では，肺野の透過性亢進，横隔膜平低化などが特徴である．胸部CTでは，肺気腫病変が低吸収領域として描出される．

検査としてはスパイロメトリーが確定診断においても，また重症度分類においても重要となる（図1参照）．その他，短時間作動型気管支拡張薬の吸入による気道可逆性試験は喘息との鑑別に有用である．

5）治療，患者指導，ケアのポイント

禁煙はCOPDの症状の進行を最も効果的に抑えると

How to activate clinical management of the aged patients using COPD guidelines?

Takahide Nagase：東京大学大学院医学系研究科呼吸器内科学

0:リスクを有する状態	スパイロメトリーは正常 症状(咳、喀痰)あり
Ⅰ:軽症COPD	FEV1/FVC＜70% FEV1≧80%予測値 症状(咳、喀痰)を伴う、または伴わない
Ⅱ:中等症COPD	FEV1/FVC＜70% 50%≦FEV1＜80%予測値 症状(咳、喀痰)を伴う、または伴わない
Ⅲ:重症COPD	FEV1/FVC＜70% 30%≦FEV1＜50%予測値 症状(咳、喀痰)を伴う、または伴わない
Ⅳ:最重症COPD	FEV1/FVC＜70% FEV1＜30%予測値、 またはFEV1＜50%予測値かつ慢性呼吸不全

COPDの重症度分類と治療指針 —GOLDガイドライン2003に基づく—

図1　ガイドラインによるCOPD重症度分類

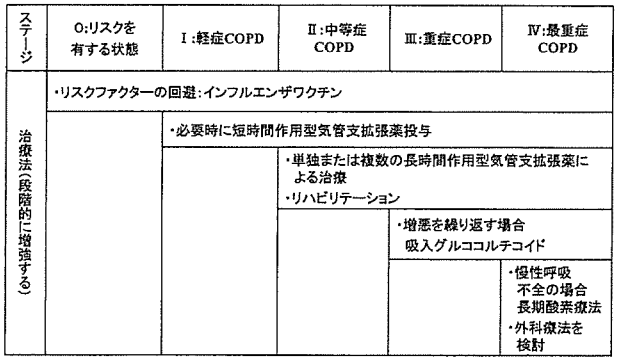

COPDの重症度分類と治療指針 —GOLDガイドライン2003に基づく—

図2　ガイドラインによるCOPD標準的治療法

され，患者教育により禁煙などのリスクファクターを減らすことは肝要である．受診時に毎回短いカウンセリングを行い，依存性がみられる例ではニコチン置換療法を行うことがよいとされる．

長期的な呼吸機能の低下を抑えると証明されている薬物はないものの，適切な薬物を用いて症状を緩和することはQOLの向上のためにも重要なことである．また，喘息と異なり，COPDは通常慢性進行性の病気なので，副作用などがない限り症状の改善がみられた薬を中止することはなく，症状の進行に伴い新たに薬を加えるstep-wise方式を取る．以下にガイドライン掲載の標準的治療法を挙げる（図2）．

Stage 0（危険性あり）以上：インフルエンザワクチンの投与が推奨される．特に高齢者では重要である．

Stage I（軽度COPD）以上：間歇的な症状がある患者に対し，短期間作動型の吸入気管支拡張薬を頓用とする．第2選択薬として徐放性テオフィリン製剤が挙げられている．

Stage II（中程度COPD）以上：短期間作動型吸入気管支拡張薬の頓用で適切な症状コントロールが得られない場合には，まず長期間作動型吸入気管支拡張薬を常用し，それで不十分であれば，テオフィリン製剤を加える．また，運動療法・栄養指導・患者教育からなる呼吸リハビリテーションを呼吸訓練士・栄養士・理学療法士などと協力しておこなう．

Stage III（重度COPD）以上：例えば3年に3回以上の反復する急性増悪を認める場合には，吸入ステロイドを常用することで，急性増悪の頻度を減らし，全身状態を改善することができる．

Stage IV（最重度COPD）：慢性呼吸不全例では酸素療法を行い，また外科的療法を考慮する．

高齢者診療におけるCOPDの重要性

近年，本邦においてもCOPDの重要性が注目されるようになった．COPDの病因として最も重要なものが喫煙であり，また喫煙者におけるCOPD発症率は年齢とともに増加する．1960年代以降，我が国におけるタバコ販売量が増加し，現在も高水準にある．厚生労働省から公表された「慢性気管支炎及び肺気腫」による死亡率は，1980年代より急増しており，約20年のタイムラグがある．高水準のタバコ販売量と人口高齢化という状況にあって，今後，益々，我が国のCOPD患者数が増加することが予想されるであろう．高齢者診療におけるCOPDの重要性は益々高まり，今後は，高齢者COPD診療のあり方がガイドライン改訂にも重要な影響を与えることが予想される．

Medical Practice

2006 vol. 23 no. 6 別冊

明らかになったわが国のCOPD患者数

長瀬隆英

東京 文光堂 本郷

明らかになったわが国のCOPD患者数

長瀬隆英
東京大学大学院医学系研究科呼吸器内科／ながせ・たかひで

概　要

慢性閉塞性肺疾患 chronic obstructive pulmonary disease(COPD)は，日本呼吸器学会のガイドライン[1]によれば，「有毒な粒子やガスの吸入によって生じた肺の炎症反応に基づく進行性の気流制限を呈する疾患」と定義されている．また，国際的にも，COPDに対する統一ガイドラインであるGlobal Initiative for Chronic Obstructive Lung Disease(GOLD)[2]により，同様に定義されている．

世界的には，COPDは疾患別死因の第4位となっており，COPD患者数はさらに増大しつつある．また，COPDに対する医療コストの増加(米国では年間4兆円と見積もられている)も重要な課題とされる．COPDに対する医療費は，症状が進むにつれ急激に増加することが指摘されており，「早期に適格な」治療介入を行うことは社会的にも大きな利益があると考えられる．

従来のCOPD患者数報告

近年，わが国においてもCOPDの重要性が注目されるようになった．COPDの病因として最も重要なものが喫煙であり，また喫煙者におけるCOPD発症率は年齢とともに増加する．**図1**に示すように，1960年代以降，わが国におけるたばこ販売量が増加し，現在も高水準にある．厚生労働省から公表された「慢性気管支炎および肺気腫」による死亡率は，1980年代より急増しており，約20年のタイムラグがある．高水準のたばこ販売量と人口高齢化という状況にあって，今後，ますます，わが国のCOPD患者数が増加することが予想されるであろう．

さて厚生労働省の患者調査によれば，1999年のCOPD患者数は20万人台とされ，COPD有病率は約0.2%程度となる．一方，欧米での疫学調査によれば，各国のCOPD有病率は約6%程度と報告されている．すなわち日本の喫煙率が欧米諸国より高いにもかかわらず，COPD有病率は著しく低いということになる．このことを説明するために人種の差などがあげられてきたが，やはり理由として不十分であることは否めないであろう．

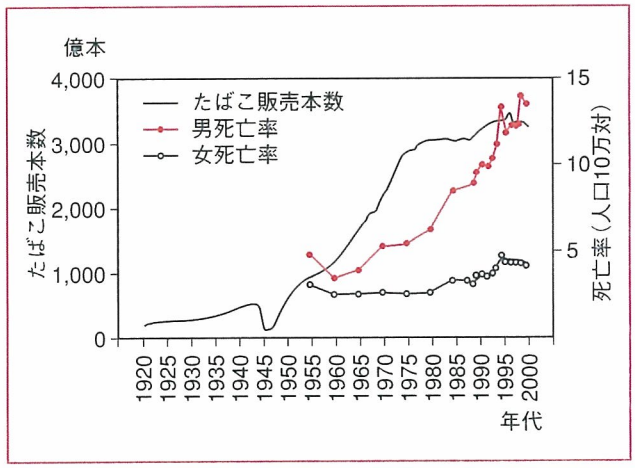

図1　日本におけるたばこ販売本数，慢性気管支炎および肺気腫*死亡率(人口10万対)の性別年次推移
(文献1)より改変引用)

最近のCOPD疫学調査

そこでわが国におけるCOPD患者数の実態を明らかにするため，住民調査によるCOPD疫学調査が実施された．この調査は，Nippon COPD Epidemiology study(NICE study)として，2000年度に全国の35施設で行われた[3]．これは，人口構成比にマッチするよう無作為に抽出された40歳以上の一般住民に対して，健康調査表記入とスパイロメトリーの参加を募ったものである．対象は男性1,383名，女性1,283名の計2,666名(平均年齢58歳)で，喫煙中の喫煙者30%，既喫煙者23%であった．スパイロメトリーで$FEV_{1.0}$/FVC < 70%をCOPDと定義すると，対象者全

1345-1551/06/¥100/頁/JCLS